Characterization of Local Field Effect in Organic Film Using Pressure Technique

by

Wendi Chang

B.S., B.A., University of Rochester (2011)

Submitted to the Department of Electrical Engineering and Computer Science
in partial fulfillment of the requirements for the degree of

Master of Science in Electrical Engineering and Computer Science

at the

MASSACHUSETTS INSTITUTE OF TECHNOLOGY

June 2013

Author .....
Department of Electrical Engineering and Computer Science
May 15, 2013

Certified by .....
Vladimir Bulović
Professor of Electrical Engineering
Thesis Supervisor

Accepted by .....
Leslie A. Kolodziejski
Chairman, Department Committee on Graduate Theses

Characterization of Local Field Effect in Organic Film Using Pressure Technique

by

Wendi Chang

Submitted to the Department of Electrical Engineering and Computer Science
on May 15, 2013, in partial fulfillment of the
requirements for the degree of
Master of Science in Electrical Engineering and Computer Science

Abstract

This thesis proposes and demonstrates a pressure probing technique for studying the effects of local dielectric changes on the excitonic energy levels in amorphous organic thin films for optoelectronic device applications. Compression of organic films causes a decrease in intermolecular spacing and, through solvation effects, lowers the exciton transition energy. A series of steady-state photoluminescence (PL) measurements performed on doped organic thin films demonstrated the applicability of pressure probing in measuring solvation effects, and fitted to solvation theory. Since a pressure probing technique eliminates composition differences and sample-to-sample variability, in comparison with doping methods, it may be a simpler method of observing energy shifts in solvation effects. Further investigation into spectral diffusion for films under compression indicates a change in spectral diffusion rate due to change in molecular packing density. Comparisons were made between spectral diffusion rates for films under pressure and films of different doping concentrations. Initial measurements of pressure effects on exciplex charge-transfer states in bulk heterojunction films are performed to show change in emission lifetimes. This work could provide a better understanding of the singlet-triplet exciton coupling rates and have a significant impact on device optimization for organic light-emitting diodes (OLEDs) and solar cell applications.

Thesis Supervisor: Vladimir Bulović
Title: Professor of Electrical Engineering

Acknowledgments

"Life is infinitely stranger than anything which the mind of man could invent."

- Sherlock Holmes, (Sir Arthur Conan Doyle, *A Case of Identity*)

I would like to express my sincere gratitude to my advisor Prof. Vladimir Bulović for his guidance, expertise, and patience as I dove head first into the strange world of organic materials. Not only was he a mentor in research, but also a role-model; I still have much to learn from his cheerful and open personality.

Vladimir provided this wonderful opportunity to work among the many brilliant minds here in Organic Nanostructured Electronics Laboratory (ONElab). Many thanks goes to our Team Awesome, which provided a research support group for those confusing times when experiments do not go as planned. I would like to especially thank Gleb and Dan, whose contributions to our collaborative works cannot be overlooked.

I would also like to thank Prof. Marc Baldo for his invaluable insights and fresh perspective on my projects. I eagerly anticipate working on future projects with him.

On a more personal level, I am grateful to all the people of ONElab for all the dinners and gatherings, for the late night games of "Bang!", and for creating a comfortable and fun work environment. I look forward to spending the rest of my graduate career with some of these lovable people. I would like to especially thank Farnaz for being a great friend. The many conversations and humorous stories we shared helped to keep me sane.

In addition, I would like to thank my family, who has been behind me in every decision I made. Their love and encouragements have helped me become who I am today. Last, but definitely not least, I would like to thank Patrick for all his love and support for the past 5 years. Through life's strange coincidences, we met at a fortuitous place and at an opportune time. Now, I cannot imagine my life any other way.

Contents

List of Figures

List of Tables

Chapter 1

Introduction

Significant technological progress in organic semiconducting materials has led to their commercialization in the forms such as organic LED (OLED) displays, solid state lighting, and photovoltaic. To support these developments, recent research efforts have focused on fundamental processes purposed for applications such as light-emitting devices [3, 4], solar concentrators [5, 6], and organic lasers [7, 8]. In contrast with inorganic semiconductor devices, Si-based devices being most prevalent, which operate based on minority and majority carriers, organic semiconductors operate based on excitons, or bound electron-hole pairs. Thus, to envision the next generation of organic electronics, a complete understanding of exciton energies and interactions is necessary.

1.1 Motivation

The optimization of organic optoelectronic devices is rooted in the fundamental understanding of the physical system. Often, a host:guest doping system is selected for desirable device characteristics such as efficiency, fabrication methods, and energy tunability [5, 7, 9]. Dicyanomethylene (DCM) class dyes are used extensively as the dopant molecules in many such applications [6, 8, 10]. To understand physical phenomenon in exciton optoelectronics and provide better device performance, the fundamental physical effects of solute-solvent interaction is crucial.

Pressure techniques have been used in various applications in organic research, ranging from sensor applications [11] to studying mechanical properties in both bulk materials [12] and thin films [13]. However, it has also proven to be a useful tool in understanding exciton energetics and molecular scale interaction with many potential applications [14, 15]. Previous research considered the effect of pressure on devices such as transistors [16] as well as films of polymers to understand the effect of molecular compression [17].

This work proposes and demonstrates the use of pressure technique for exciton energy tuning due to solvation effects. The objective is to employ an accepted technique in a novel application to probe organic material properties and exciton physics, and offer an additional accessible parameter for tuning exciton energy.

1.2 Local Field Effects

On a molecular scale, a localized electron-hole pair is usually confined to a single molecule; this bound pair is known as a Frenkel exciton. Both the excited state and the ground state of the molecule have certain electronic charge distributions across the molecule, and are often modeled as dipoles. These dipole-dipole interactions between molecules create a local electric field effect that is often characterized as a reaction field, separate from any external electric field. These effects are important in considering the perturbation on excitonic energy levels. With a better understanding of local field effects, it is possible to controllably tune the band-gap energy of the organic material, to better optimize optoelectronic devices. This solvation effect has been studied through PL measurement in doping techniques for applications such as OLEDs [1, 5, 9, 18, 19]. Recent works on OLEDs show that different emission wavelengths can be achieved for the same OLED material by simply varying relative doping concentrations as shown by the CIE color plot in Figure 1-1.

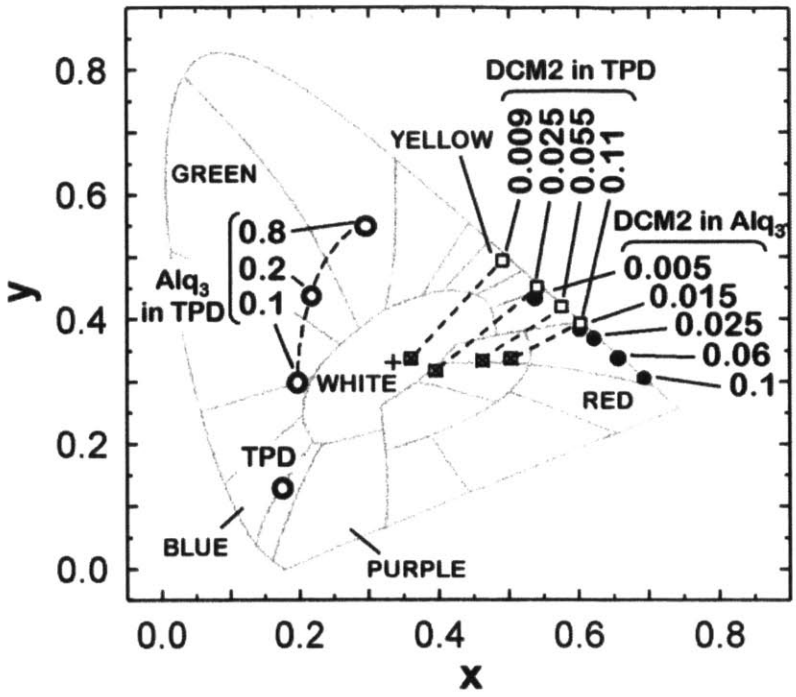

Figure 1-1: CIE plot of OLED emission of different material systems at various doping concentrations by percent weight. [1]

Previous work on the solid state solvation effect (SSSE) focused on the ability to tune peak emission by varying guest doping molecule concentration. Bulović and colleagues reported up to 75 nm tuning of emission through doping of laser dye 4-(dicyanomethylene)-2-methyl-6-(julolidin-4-ylvinyl)-4Hpyran) (DCM(II)) in tris(8-hydroxyquinoline) aluminum (Alq_3) and N,N-diphenyl-N,N-bis(3-methylphenyl)-1,1-biphenyl-4,4-diamine (TPD) films for OLED applications [1]. They have also reported a 40 nm shift in peak PL for 0.005% DCM(II) molecules in polystyrene (PS) and varied the local dielectric by tuning doping levels of camphoric anhydride (CA) [18]. This effect is not limited to OLEDs, and recent work by Green *et al.* used similar SSSE doping methods for efficient luminescent solar concentrators [5].

However, doping techniques have significant sample variability and changes in film composition create extra variables. Rather than trying to consider the effects of all the relevant variables of a complex system, it may be possible to simplify the problem

by employing an alternative technique. This led to the the proposition of observing SSSE due to simple compression of the film by measuring exciton PL emission.

1.3 Description of Experimental Setup

The experimental setup for general steady-state and time resolved PL spectrum measurements is shown in Figure 1-2.

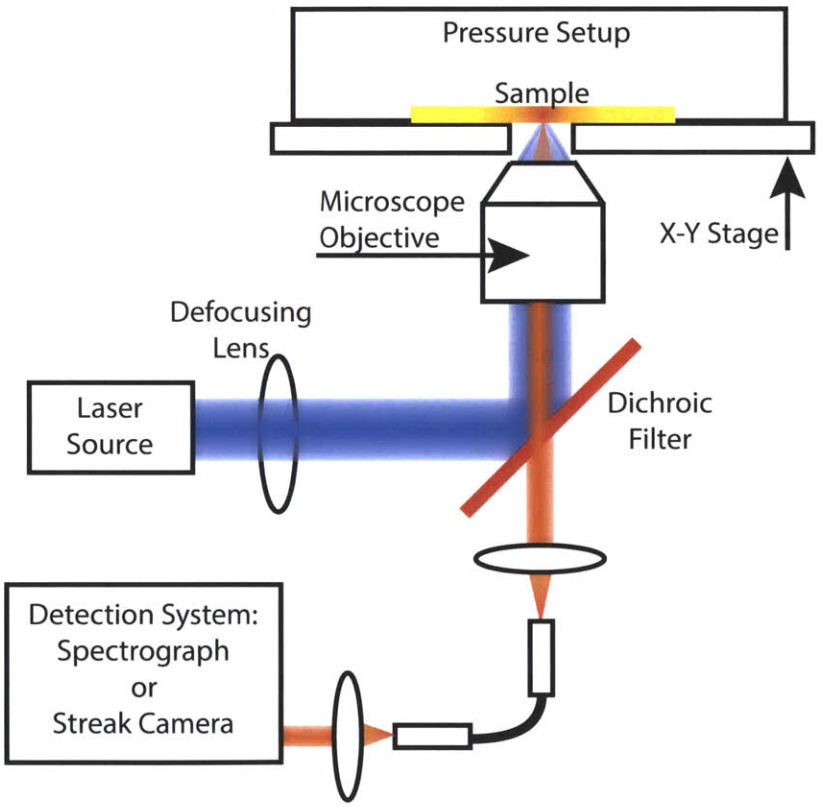

Figure 1-2: Schematic of experimental system with simplified illustration of optical components.

A measurement sample is place on the microscope stage under a mechanical pressure setup. A wavelength-tunable laser (using a optical parametric amplifier) is coupled into the microscope, with defocusing lens controlling excitation spot size. The microscope objective both focuses an excitation laser onto the film and captures sub-

sequent exciton emission. A dichroic filter of appropriate transmission and reflection is used to reflect excitation wavelengths and transmit sample emission wavelengths. The output of the microscope is either free-space coupled or fiber-coupled to a spectrograph for steady-state PL or a streak camera for time-resolved PL (TRPL).

1.3.1 Mechanical Setup

The mechanical pressure setup, shown in Figure 1-3, is clamped onto the microscope stage. The setup includes force and sample position scanning capabilities as well as optical accessibility for PL measurement. The microscope x-y stage supports the pressure setup and moves relative to the excitation laser spot for sample scan. In order to scan pressure, force is applied through a steel probe of contact diameter of approximately 200 μm. Mechanical springs are inserted between the probe and a motorized micrometer to create a linear force-displacement relationship. Applied pressure is estimated from linearized force and approximate contact area. Using the motorized micrometer, the max pressure applied is around 0.5 GPa. A manual micrometer can also be installed to apply a greater range of pressure, which will then be limited by sample durability and possible unaccounted distribution of compression in the mechanical components. The estimated pressures have a systematic error of $\sim$ 0.1 GPa resulting from the contact area approximation.

1.4 Outline

This thesis is divided into 6 chapters:

- Chapter two includes an overview of solid state solvation theory and derives theoretical expressions used in later experimental comparisons.
- Chapter three describes experiments on steady-state exciton photoluminescence (PL) of doped organic films under pressure.
- Chapter four provides spectral time-resolved photoluminescence (TRPL) of

doped organic films under pressure, and direct comparison with doping-variable study.

- Chapter five describes pressure experiments on charge-transfer state (CT), namely an exciplex state, in thin-film bulk heterojunction for device applications.
- Chapter six includes future works and concluding remarks.

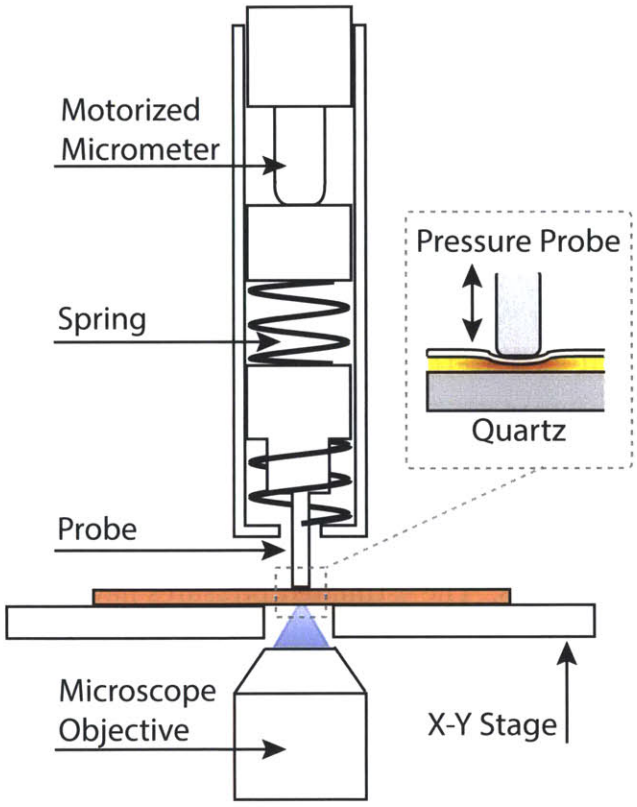

Figure 1-3: Experimental setup for *in situ* optical measurement of organic thin film sample under mechanical pressure.

Chapter 2

Solid State Solvation Effect

The solvation effect, as pertains to organic molecules, describes the physical reorientation of surrounding solvent molecules due to a change in solute dipole moment during absorption or emission, which in turn perturbs the exciton transition energy. This effect has long been observed in liquid state by a simple phenomenon of different color emission of the same dye molecule dissolved in various solvents [18, 19, 20].

Figure 2-1 shows measured PL of DCM dye dissolved in common organic solvents.

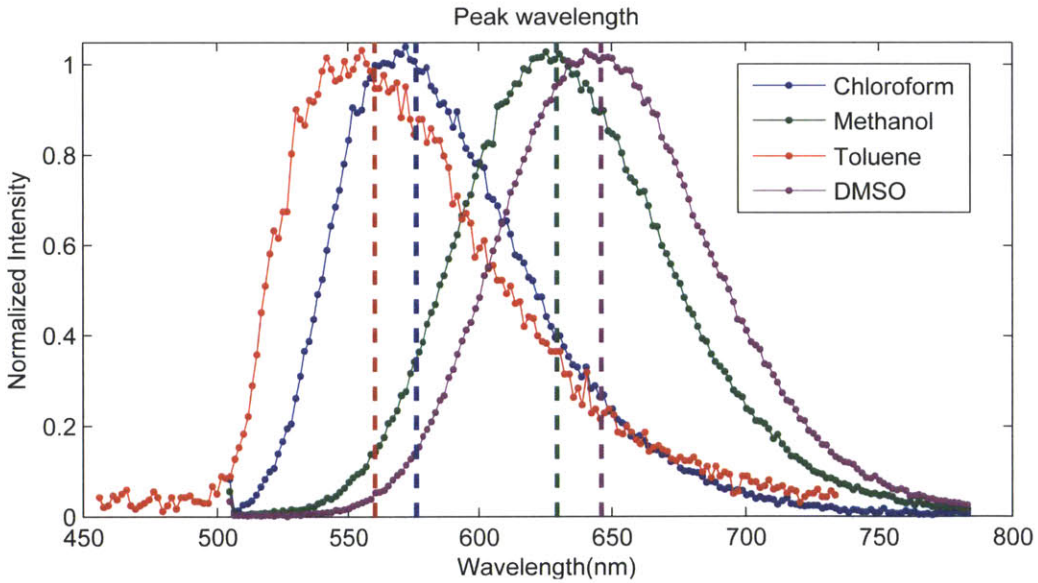

Figure 2-1: Shift in PL for DCM molecules dissolve in select solvents. The peak emission changes due to different solvent dielectric constants

As consistent with reported literature results [18], in Figure 2-1, the DCM peak PL emission shows a clear redshift for solvents of higher dielectric constants[1], which is summarized in Table 2.1.[2]

Solvent	Dielectric Constant	DCM Peak Emission (nm)
Toluene	2.38	560
Chloroform	4.81	576
Methanol	32.70	623
Dimethyl sulfoxide	46.68	646

Table 2.1: Dielectric constants and dissolved DCM peak emission in select solvents

Further study in solid state showed that through molecular doping, the same local dielectric field effect is observed by simply having more neighboring dye molecules as part of the solvent environment. The gross movement in solvent dipole alignment affects the excitonic energy states, both ground and excited, which affects the transition energy. Because this effect is dependent on the dipole moment of the guest dye molecule, the shift in transition energy may be a bathochromic (red) shift or a hypsochromic (blue) shift. For typical dyes, the transition dipole is aligned such that for increasingly polarizable solvent environments a bathochromic shift in transition energy is observed, termed positive solvatochromism as illustrated in bottom schematic of Figure 2-2. The reaction electric field from solvent reorientation allows an energy relaxation in typical solute molecules with large transition dipole moments. DCM class dyes are one such example, which exhibits the characteristic red shift. There are molecules such as the merocyanine dyes, which would exhibit the negative solvatochromism effect and a hypsochromic shift is observed for increasing polarizable solvent [19].

As mentioned in the previous chapter, although doping studies showed clear SSSE,

[1] http://macro.lsu.edu/HowTo/solvents/Dielectric%20Constant%20.htm

[2] For intellectual curiosity, the same PL measurements of DCM dissolved in various deuterated form of the select solvents were performed. The peak PL emissions were found to be the same within spectrum resolution for each solvent and corresponding deuterated solvent. As discussed later in this chapter, these results suggest that solvation effect is dominated by factors such as dielectric constant and dipole moment of solvent, which is not effected by deuteration.

to further our understanding of local dielectric effects on energy states, a new technique is necessary which eliminates variables introduced in composition differences and sample-to-sample experimental variations. In this effort a pressure technique was employed, which can cause film deformation and decrease intermolecular distance. This decrease in molecular spacing effectively created different local dielectric solvent environments using a controlled external parameter, as illustrated in the top images of Figure 2-2)

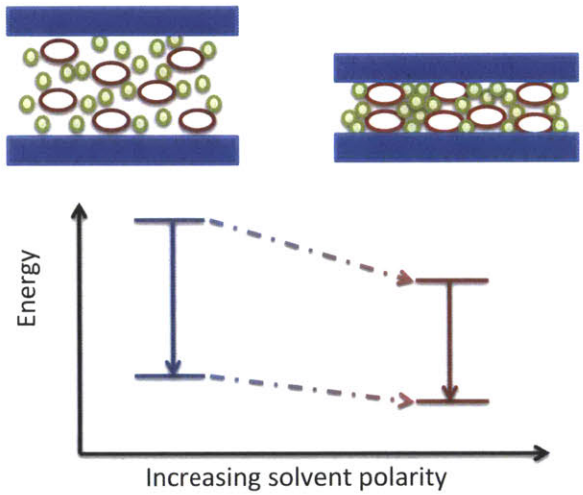

Figure 2-2: Solvatochromism: (top) change in molecular spacing to change polarizability, (bottom) bathochromic shift in transition energy for increasing polarizable medium for typical dye molecule, or positive solvatochromism.

2.1 Solvation Theory

To model the solute dipole interaction with surrounding solvent media, consider a dielectric continuum model with a few standard assumptions as consistent with the Onsager model for liquid state solvation effects [21]:

- solute electronic densities are reduced to dipoles
- solute molecules are enclosed in spherical cavities, and are only affected by neighboring molecules within a certain constant radius, a

A dipole as a first order approximation of the electron density is a fairly accurate description of the dye molecules used in this work [20]. The second assumption was an implicit approximation of the solvent environment. There are many alternative models in capturing a more accurate system using explicit methods or a combination, and variations on cavities and solute modeling exist to make model selection nontrivial [22]. This work focused on the spherical cavity model, which simplified much of the computation and still gives a reasonable representation of the energy shifts. To calculate the change in transition energy, consider the dipole moments of the solute and the reaction field created by the Frank-Condon effect upon absorption. This reaction field $E_{reaction}$ is dependent on the polarizability of the solvent and the corresponding solute static dipole moment for the ground and excited states. Thus a simple Stark perturbation on the energy is given by $\Delta E = -\vec{\mu} \cdot \vec{E}_{reaction}$. Considering all the factors, the change in the transition energy as measured by emission according to Ooshika-Lippert-Mataga (OLM) solvation theory is expressed as [23, 24, 25, 26]:

$$\Delta \mathrm{E_{PL}} = -\frac{\Delta\vec{\mu}}{a^3} \cdot \left(\Lambda(\epsilon)\vec{\mu}_e + \Lambda\left(n^2\right)\vec{\mu}_g\right) \tag{2.1}$$

$$\Lambda(\epsilon) = \frac{2(\epsilon - 1)}{2\epsilon + 1} \tag{2.2}$$

The solvent polarizability is manifest in two different capacities: the nuclear reorientation $\Lambda(\epsilon)$ and the electron reorientation $\Lambda(n^2)$. Note that this transition energy was calculated for molecular emission, and the Franck-Condon shift in energy due to molecular orientation was taken in to account. A similar expression could be derived for the absorption transition energy. However, experimentally, solvatochromism is easier measured in emission rather than absorption due to the time response of solvent reorientation compared to photon absorption time scales. To further simplify the system to have a direct relationship between change in transition energy and density, a few more assumptions were included:

- the solute electron reorientation term $\vec{\mu}_g\Lambda(n^2)$ is negligible with respect to the nuclear reorientation term

- solute molecule dipole moments are constant with pressure

The high frequency solvent electron reorientation term is approximately on the same time scale as solute absorption and emission with some contribution to the solvation effect. Since the dipole moment of the ground state of DCM is almost 5 times less than that of the excited state [20], any effect due to change in density would be dominated by the first term. Thus, the contribution of the second term was assumed to be relatively invariant as a function of pressure compared to the low frequency solvent nuclear reorientation term. The second assumption specifies that the dipole moments of the excited state $\vec{\mu}_e$, ground state $\vec{\mu}_g$, and transition $\Delta\vec{\mu}$ were only dependent on the doping molecule properties and were also constant with pressure. These assumptions result in a simple relationship of change in transition energy as a function of local dielectric constant [18]:

$$\Delta \mathrm{E_{PL}} \approx -\mathrm{A}\Lambda(\epsilon) + C \tag{2.3}$$

We used the relationship of $\chi = \epsilon - 1$ to find the relationship between the change in dielectric susceptibility from its initial value and the change in transition energy.

$$\Delta \mathrm{E_{PL}} \approx -A\left(\frac{2\chi}{4\chi+3}\right) + C = -A\left(\frac{2\chi_m(1+\Delta\chi)}{4\chi_m(1+\Delta\chi)+3}\right) + C \tag{2.4}$$

Note that $\epsilon_m = \chi_m + 1$ is simply the bulk dielectric constant of the host-guest system under zero pressure. For example, polystyrene (PS) with 0.5% doped DCM(II) has $\epsilon_m = 2.44$ [18]. From here, the constants A and C are found for specific dye molecules by simply fitting the peak PL emission energy of the dye dissolved in various liquid solvents as a function of dielectric constants, for which there exist an abundance of published works for most common organic dyes. Such fitting of DCM(II) dye in liquid state studies will give the values: A = .55 eV, C = 2.4 eV [18], and the transition energy as a function of dielectric is plotted in Figure 2-3.

Further approximations were necessary to relate these theoretical results to experimental values. A first order consideration of the relationship between the density of molecules and dielectric susceptibility revealed a direct proportionality, such that

a percent change in density would be directly reflected in a percent change in susceptibility, $\Delta N(\%) = \frac{\Delta N}{N} = \frac{\Delta \chi}{\chi} = \Delta \chi(\%)$. Now, we have a direct relationship between change in film density and change in emission energy. Since pressure P was applied in only one dimension, the change in density is the change in linear strain in the axis of applied stress. Thus, the fit to theory for the pressure-dependent experimental results is a simple relationship as expressed below, where the elastic modulus of the material E_m is used as a fitting parameter:

$$\Delta \mathrm{E_{PL}} \approx -A\left(\frac{2\left(\epsilon_m - 1\right)\left(1 + \Delta \mathrm{N}\right)}{4\left(\epsilon_m - 1\right)\left(1 + \Delta \mathrm{N}\right) + 3}\right) + C \approx -A\left(\frac{2\left(\epsilon_m - 1\right)\left(1 + \frac{P}{E_m}\right)}{4\left(\epsilon_m - 1\right)\left(1 + \frac{P}{E_m}\right) + 3}\right) + C \tag{2.5}$$

This expression will be useful in comparing the steady-state PL results with theory.

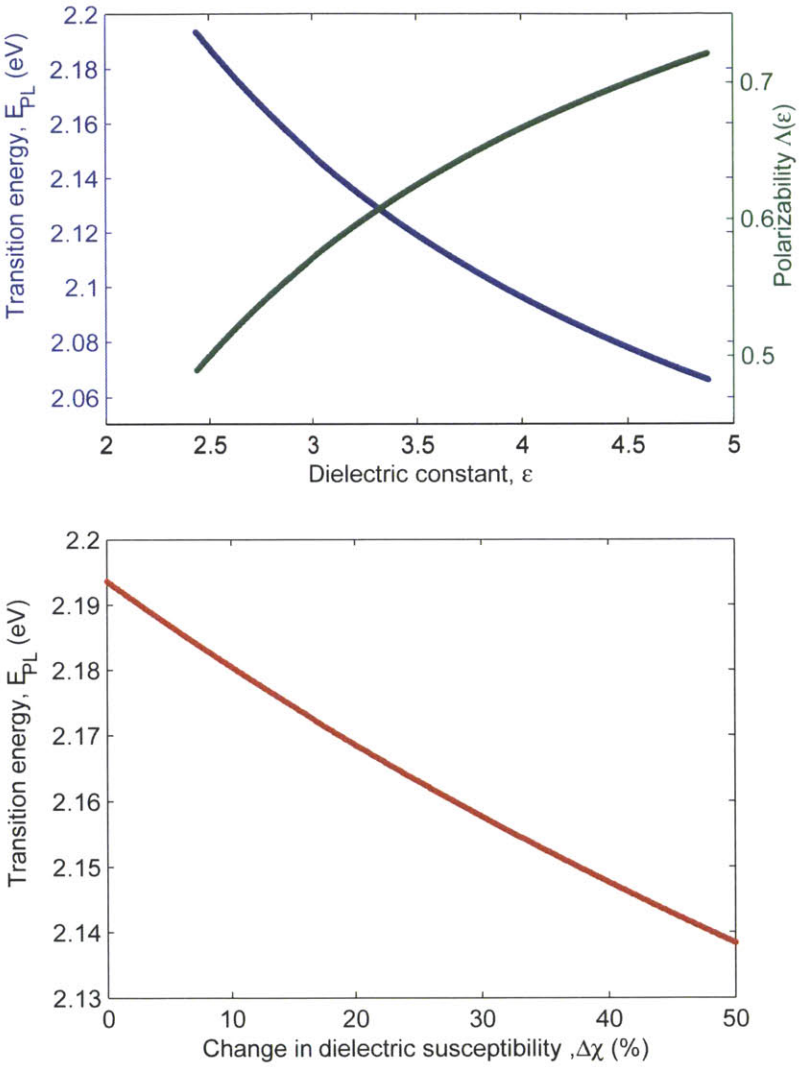

Figure 2-3: DCM(II) emission transition energy shift as predicted by OLM theory: (top) the theoretical prediction of the emission transition energy (on the left axis in blue) and the solvent nuclear polarizabilty (on the right axis in green) as a function of dielectric constant for DCM(II); (bottom) the same transition energy as a function of the percent change in dielectric susceptibility from an initial solvent property of polystyrene.

Chapter 3

Steady-State Photoluminescence

Steady-state spectroscopy was performed with a common spectrograph system, which spectrally resolves the signal using a slit and grating and creates a spatial mapping of spectral data. A detector system measures the light intensity for each wavelength, in this case an array of Si photodetectors. The resolution of the spectrograph can be limited by the slit size as well as detector pixel size[1]. Photoluminescence (PL) is a standard and widely-accepted method of measuring transition energy in emission of semiconductors.

The peak PL emission of materials is often used as a measurement of the excitonic band-gap energy. However, it is important to note that the emission spectrum are dependent on factors such as the density of states and energy relaxation or transfer, thus the spectrum may be multi-peaked. To further complicated the measurement, a significant Stokes shift often exists between peak absorption and emission energies. In these organic systems, the peak energy measured is the peak emission of the organic molecules, which undergoes a Franck-Condon shift [27] to a significantly lower energy due to molecular re-orientation.

For SSSE experiments, emission of dye molecules such as DCM(II), shown in Figure 3-1, have a single peak (indicated with blue dash), which represents the most likely exciton emission transition energy. The theoretical expression derived from the

[1]In the following experiments, signal intensity was sufficiently high such that all measurements were pixel resolution limited.

previous chapter is based on emission energy; thus, PL is an accurate experimental measure of this transition. Note that due to energy transfer, the emission spectrum is slightly asymmetric with a red tail. It may be useful to also consider the centroid energy (indicated with red dash), the median energy resulting from a weighted averaging of the intensity over wavelength.

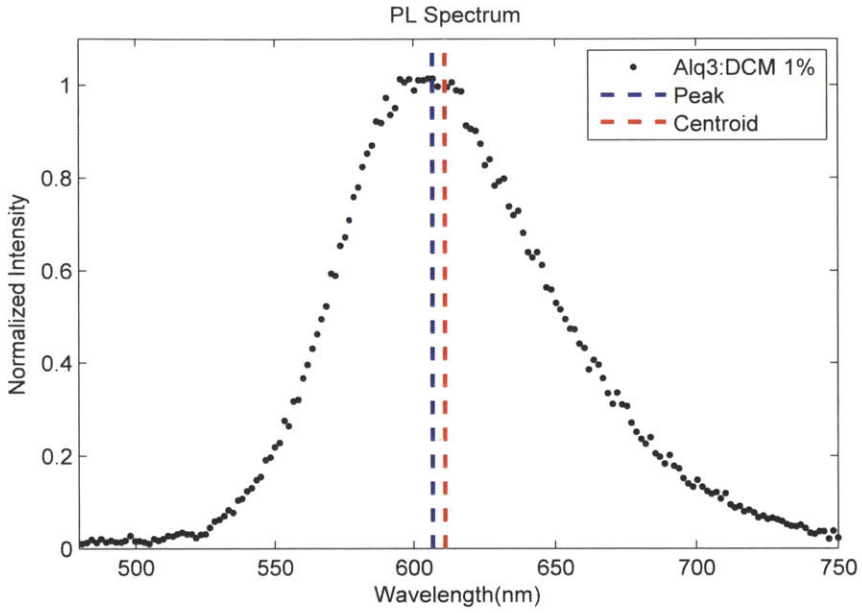

Figure 3-1: Typical Alq_3:DCM(II) (1% doping) PL emission spectrum with corresponding peak and centroid wavelength

The difference between the peak and the centroid highlights the difference between the normalized intensity PL spectral profile and a Gaussian curve[2]. The combination of the two metrics gives a better picture of any change in the emission spectrum, both peak and shape. Only the peak is used when considering the most probably bandgap energy.

[2]A Gaussian distribution has the same peak and centroid.

3.1 Sample Preparation

Samples were deposited on clean thick quartz substrates by either vacuum thermal evaporation or solution spin coating. Films of 200 nm Alq_3:DCM(II) were deposited using thermal co-evaporation at a chamber pressure below 10^{-6} Torr at a total rate of 4.0 Å/s. Sample doping concentration was controlled by calibrated relative deposition rates with doping variability within 0.5%. For example, a 1% doped film would be deposited by using DCM(II) doping rate of .04 Å/s. Films of 200 nm PS:DCM(II) were spin-cast from a 30mg/ml chloroform solution at 2000 RPM; doping concentrations were controlled by relative mass dissolved in initial solvent.

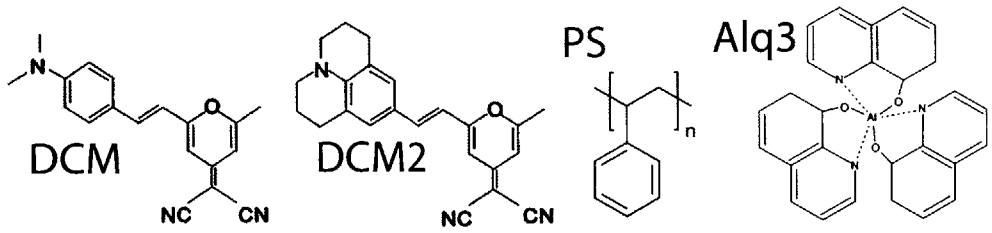

Figure 3-2: Chemical structure: DCM class dyes DCM and DCM(II), polystyrene, and Alq_3

After deposition, each sample of organic film was packaged with a clean, thin glass cover to avoid any photo-oxidation related degradation. The glass cover is flexible to allow pressure probing of the sample, but adds uncertainty in pressure by spreading the applied force.

We recorded the steady-state PL spectra using a spectrograph and Si camera detector array as shown in Figure 1-2. An excitation source of $\lambda = 475$ nm was used, where DCM(II) has large absorption and the host materials has relatively insignificant absorption; specifically, PS and Alq_3 are transparent at 475 nm [28]. For each PL spectra taken, the peak was found by fitting to a Gaussian to quantify shifts in spectra; an example peak fit is shown in Figure 3-3 as a solid black curve to find peak of PL plotted as black dots.

3.2 Spectral Results

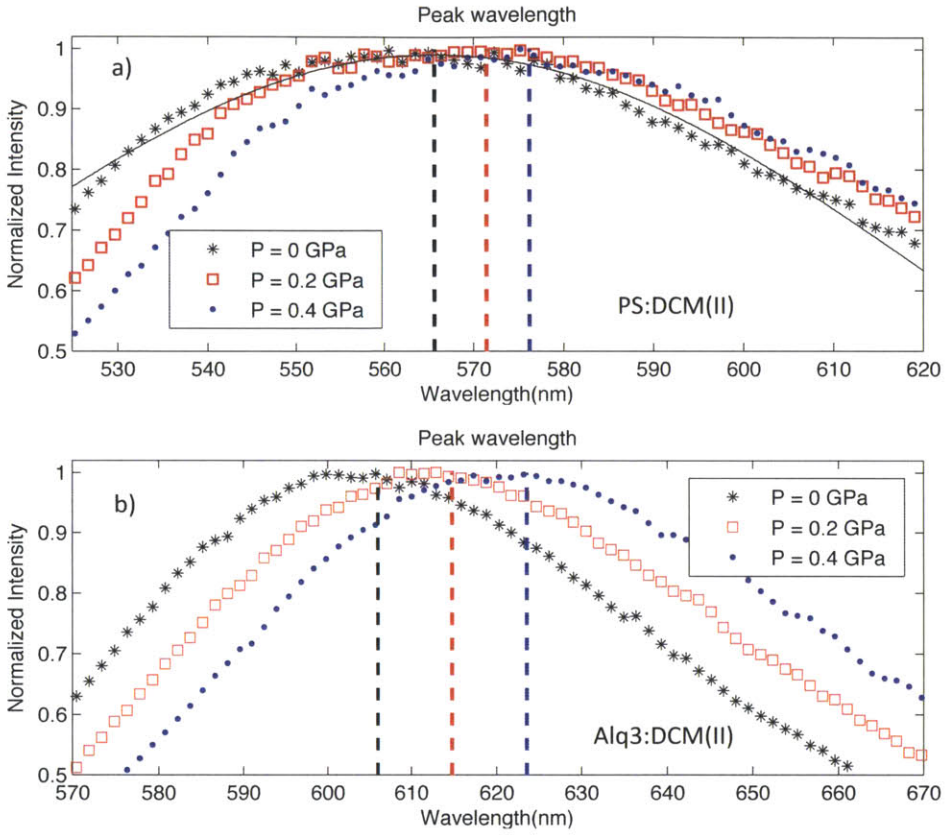

Figure 3-3: Typical PL emission spectrum shift for PS:DCM(II) at 0.5% doping (top) and Alq_3:DCM(II) at 1% doping(bottom) under pressure. The top figure shows an example Gaussian smoothing fit to find peak wavelength. The computed peak wavelengths are indicated by correspondingly colored dotted lines for each spectrum.

3.2.1 Sample Scan

We scanned a laser of spot size diameter $\sim$50 μm across the point of pressure in a sample scan to find the spectrum red shift induced by the pressure probe (Figure 3-4). Each vertical slice of the figure represents the steady-state PL spectrum with intensity shown in color-scale verses the vertical axis of wavelength. A peak wavelength was found for each spectrum and plotted as white dots overlaying the sample scan data.

A clear red shift of over 20 nm was observed under pressure.

The sample scan data suggests a possible use of pressure for exciton energy gradient on the micrometer scale. Since excitons (electron and hole pairs) are neutral in charge, diffusion studies are difficult due to lack of precise creation of energy gradients[3]. It may intriguing to consider patterned microscopic pressure probes to create shorter scale energy gradients for possible studies on excitonic diffusion, which is usually on the scale of tens of nanometers.

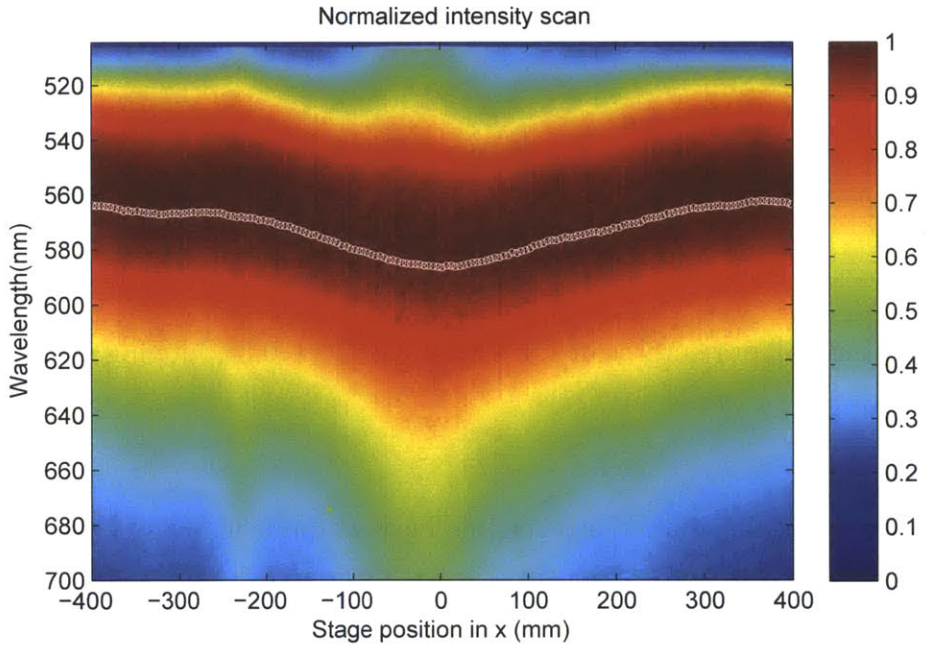

Figure 3-4: Typical sample scan for PS:DCM(II) at 0.5% doping under P $\sim$ 0.4 GPa with peak PL plotted in white. The probe makes contact around the center and is indicated by the shift in emission.

3.2.2 Pressure Scan

Pressure scans are performed by observing the PL of the film under the point of pressure as a function of micrometer displacement. A 3-D data plot similar to the sample scan data is generated for each pressure scan as shown below in Figure 3-5.

[3]Diffusion study on charged particles are often performed using electric field to create energy gradient, which is not as easily applicable in the case of excitons.

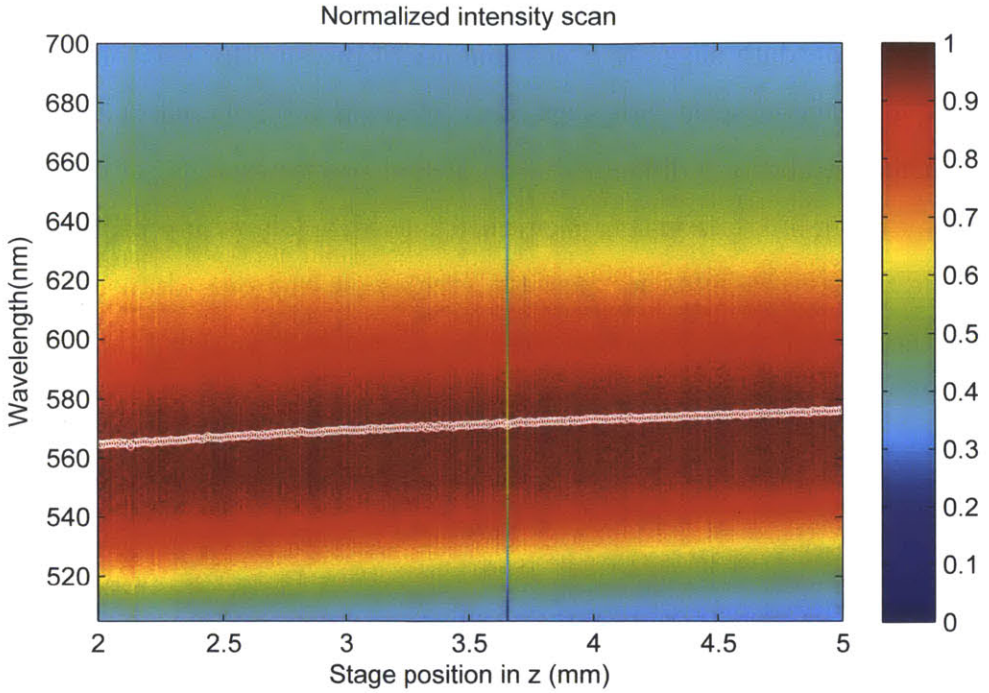

Figure 3-5: Typical pressure scan for PS:DCM(II) at 0.5% doping with peak PL plotted in white.

Pressure scan results showed a reversible bathochromic shift in peak PL emission over 15nm in samples of 200nm thin film of Alq_3:DCM(II) at 1% doping. For 200nm thin films of PS:DCM(II) at 0.5% doping, around 10nm reversible bathochromic peak shift was observed. For increasing pressure, the observed effects are consistent with increasing the concentration of guest molecules in SSSE, as expected. This indicates an increase in the local dielectric constant under compression. To confirm the spectral shift, the centroid was also computed for each spectrum. The comparison between the fitted peak and computed centroid as a function of pressure for the two different samples is plotted in Figure 3-6.

Because the spectrum of PS:DCM(II) is slightly more asymmetric with more emission in the longer wavelength tail, the difference between the centroid and the peak is larger than that of Alq_3:DCM(II). For both samples, the shifts in PL centroid are well correlated with the shift in peak emission, confirming the homogeneity spectral shifts of the sampled dye molecules.

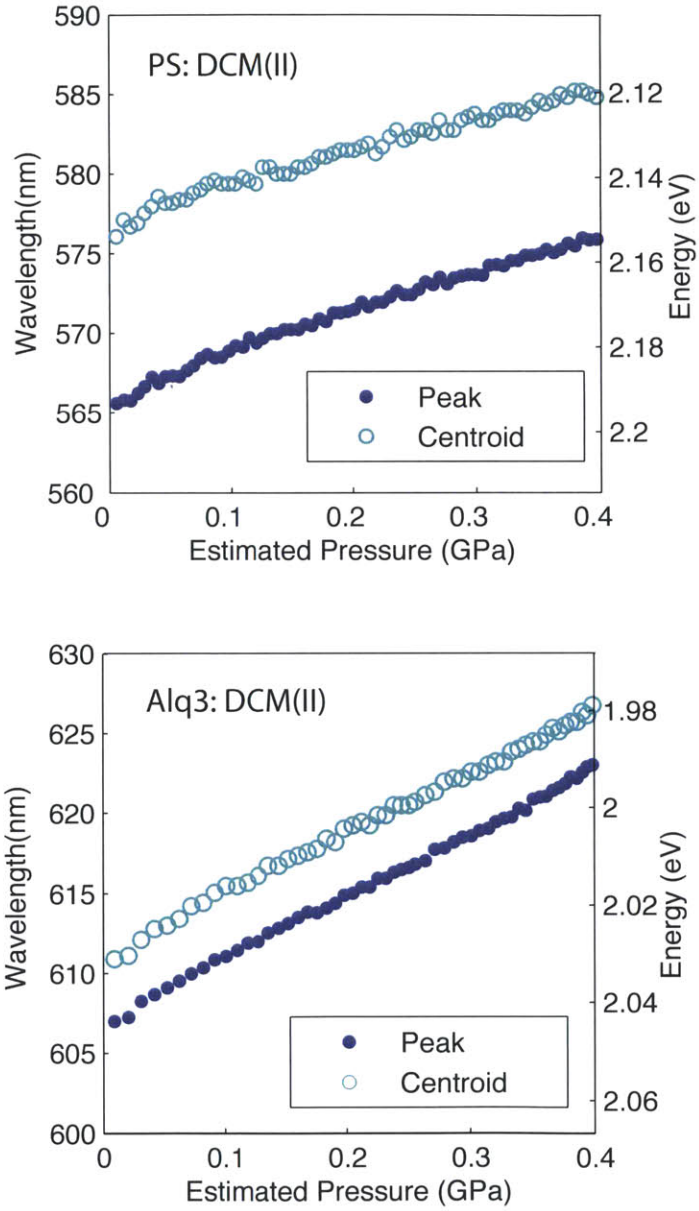

Figure 3-6: Peak and centroid wavelength shift under pressure for PS:DCM(II) at 0.5% doping (top) and Alq_3:DCM(II) at 1% doping(bottom).

3.3 Experimental Fit to Theory

The experimental PL peak energy can be now plotted with the theoretical prediction given in Equation 2.5 using the elastic modulus of the host material as a fitting parameter.

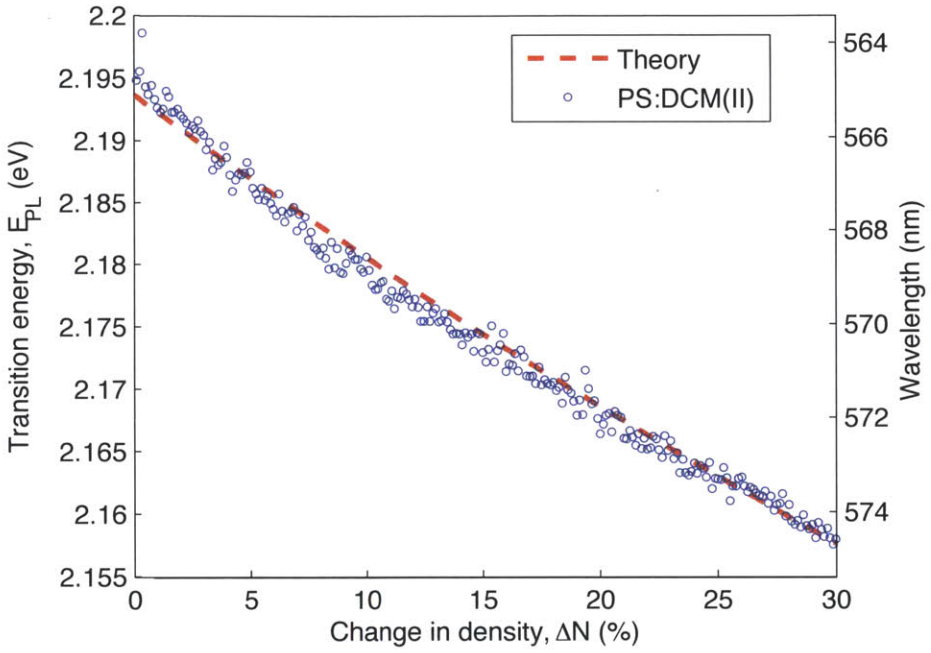

Figure 3-7: Fitting experimental results of PS:DCM(II) peak energy shift as function of change molecular packing density to simplified OLM theory using host modulus fitting parameter, resulting in $E_{PS} = 1.2 \pm 0.6$ GPa.

PS:DCM(II) experimental results fitted the simplified OLM theory as shown in Figure 3-7, with an PS elastic modulus of 1.2±0.6 GPa. This was in relatively good agreement with measured literature values [29], which confirms that the observed bathochromic shift was dominated by local dielectric effects, as expected. A similar fit was performed for the Alq_3:DCM(II) to find an estimated elastic modulus of 0.9±0.4 GPa for Alq_3 as shown in Figure 3-8. This fitted value was within error of measured modulus using standard techniques such as wrinkle-based metrology [30, 31].

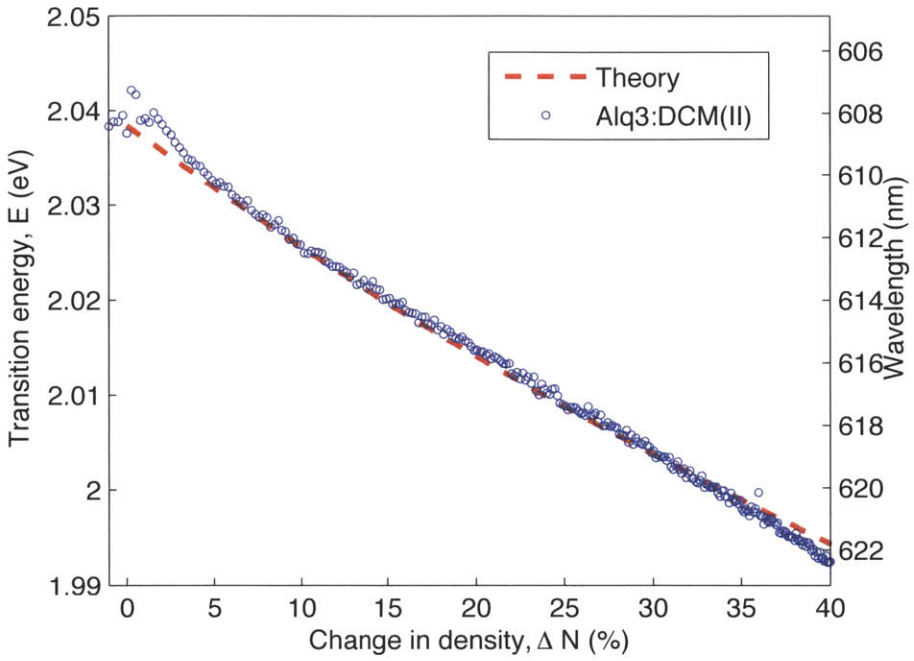

Figure 3-8: Fitting experimental data of Alq_3:DCM(II) peak energy shift to OLM theory, resulting in $E_{Alq_3} = 0.9 \pm 0.4$ GPa.

These results show that the pressure probing technique is a viable method in studying SSSE, and provides a unique parameter for exciton energy tunability. More precise pressure systems may result in a new method of measuring elastic modulus of thin amorphous organic films to corroborate established methods such as nano-indentation or wrinkle-based techniques. As mentioned, further work with patterned micro-scale probes may yield an interesting technique to study exciton diffusion, similar to pressure systems used to trap exciton-polaritons in microcavity structures [32].

Chapter 4

Time-Resolved Photoluminescence

Time-resolved PL (TRPL) is a standard technique employed to understand the time response of a material to pulsed excitation and is often used to measure exciton lifetimes in semiconductors. To fully understand the effects of compression on organic thin films, time response data is essential. TRPL comparisons between compression and doping results are made. A streak camera setup was used to obtain simultaneously time-resolved and wavelength-resolved PL data.

4.1 Streak Camera

To obtain spectral data in TRPL, one common method is a streak camera system (Figure 4-1[1]). The setup has a spectral slit and grating similar to a spectrograph. Subsequently, the spectrally resolved photons are limited by a second, orthogonal spatial slit (for temporal resolution) and are converted to electrons using a photocathode. Then, a pair of sweeping electrode deflects the electrons to create a spatial mapping of the temporal data. The electrons, spectrally separated in one dimension and temporally resolved in the other, are captured using a phosphor screen and camera setup.

The Hamamatsu streak camera system used is capable of time resolution measurements up to ps; for even finer time resolution spectral measurement, a Kerr shutter

[1]http://www.hamamatsu.com/resources/pdf/sys/e_streakh.pdf

system may be employed. For the organic materials under study, the time resolution of the streak setup was sufficient.

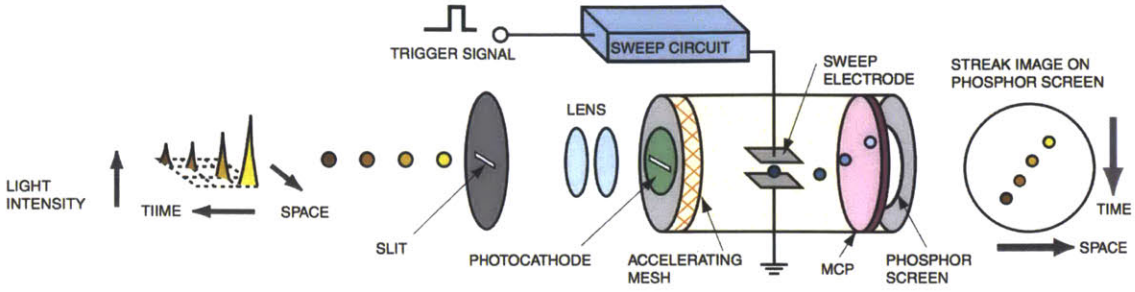

Figure 4-1: Schematic of streak camera system. Curtesy of Hamamatsu.

4.2 Wavelength- or Time-Integrated

TRPL techniques are often used to observe exciton radiative lifetime and a fast-response photo-detector may perform the same lifetime measurement in a more simplified setup. However spectrally resolved measurements could give additional insights on spectral diffusion and will be considered in the next section. In this section, we analyze the data from the streak camera using either wavelength or time integration: time integration will produce similar result as steady-state and will be a confirmation of the experimental result of the previous chapter; wavelength integration will result in the time response measurement used to determine exciton lifetime.

To fully quantify the effect of pressure, time resolve measurement of both PS:DCM(II) and Alq3:DCM are performed under select pressures. In previous works, drastic changes in lifetime were observed for host:guest organic thin films due to sample doping concentration [33]. The driving mechanism behind the change in exciton lifetime is the significant aggregation of guest dye molecules for increasing doping concentration, creating non-radiative states and quenching sites. Notably, this aggregation effect and other film composition related effects should not play a significant role in pressure techniques.

Typical steak camera measurements of PS:DCM(II) at 0.5% doping under various

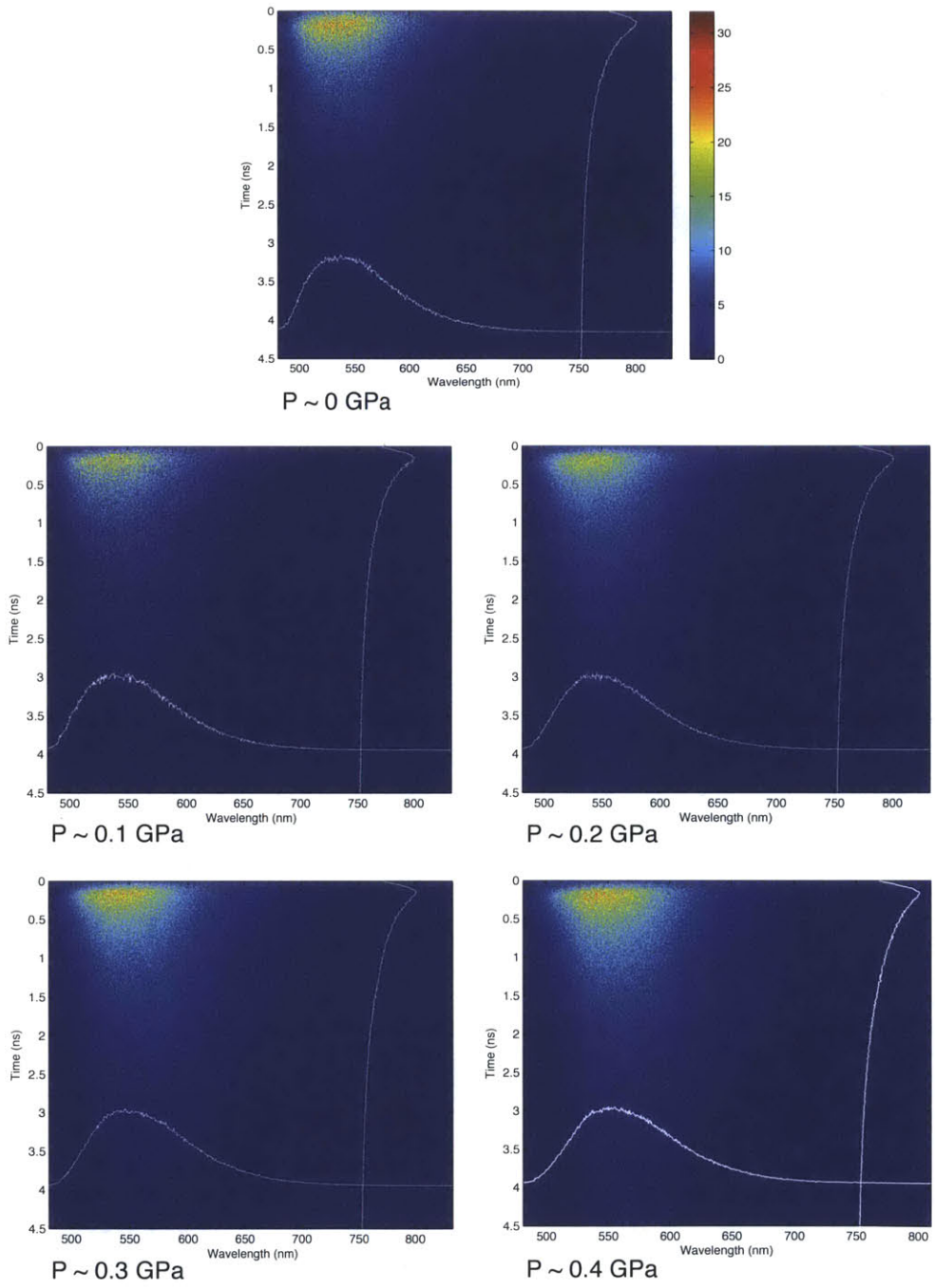

Figure 4-2: Streak camera data of PS:DCM(II) at 0.5% doping under select pressures (labeled below each figure); with time as vertical axis, wavelength as horizontal axis, and intensity indicated in color scale. The time-integrated PL spectra are plotted in white on the bottom of each figure. The wavelength-integrated time response data are plotted in white on the left of each figure.

pressures are shown in Figure 4-2. The time-integrated PL spectrum for each set of data was plotted to find the same result as the steady-state measurements; an evident red shift in peak emission was observed as consistent with the steady-state findings (Figure 4-3).

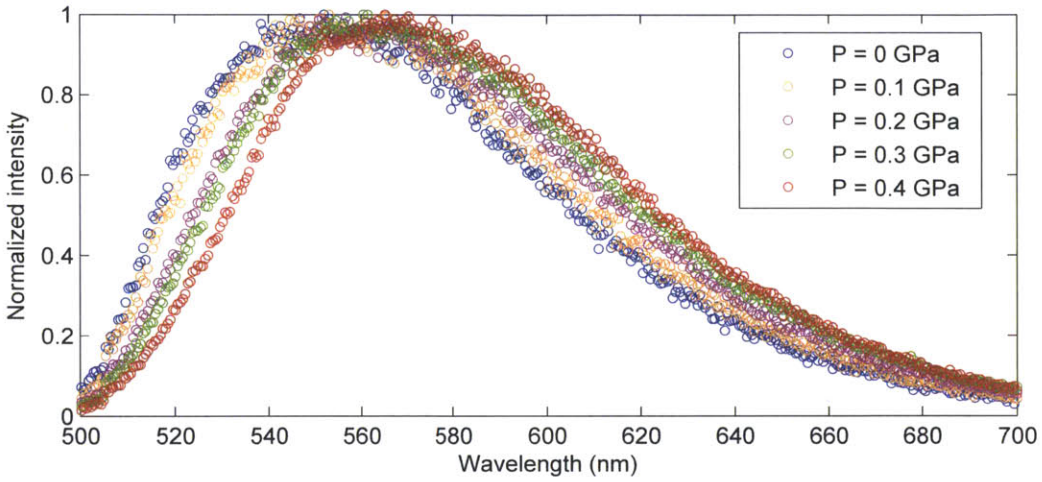

Figure 4-3: Streak camera: time-integrated PL spectra of PS:DCM(II) at 0.5% doping under select pressures.

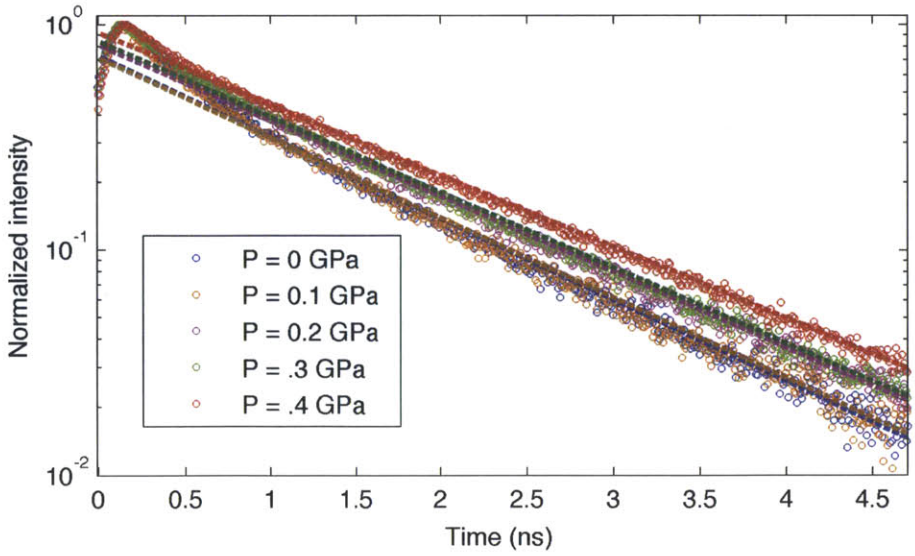

Figure 4-4: Streak camera: wavelength-integrated TRPL of PS:DCM(II) at 0.5% doping under select pressures. Intensity normalized to unity for lifetime comparison.

This confirms the steady-state trend discussed in the previous chapter. For the exciton lifetime measurements, Figure 4-4 plots the wavelength-integrated time response of the PS:DCM(II) under pressure.

Each TRPL was fitted to an exponential lifetime, which are listed in Table 4.1. Instead of a significant decrease in lifetime as expected for aggregation effects, a slight increase in lifetime was observed. This supports the supposition that pressure technique was a more direct method compared to doping experiments, where the change in composition could also contribute to a red shift in emission, the same effect as the bathochromic shift of SSSE. The sample streak camera measurements and analysis were performed for Alq3:DCM(II) films and are plotted in Figure 4-5

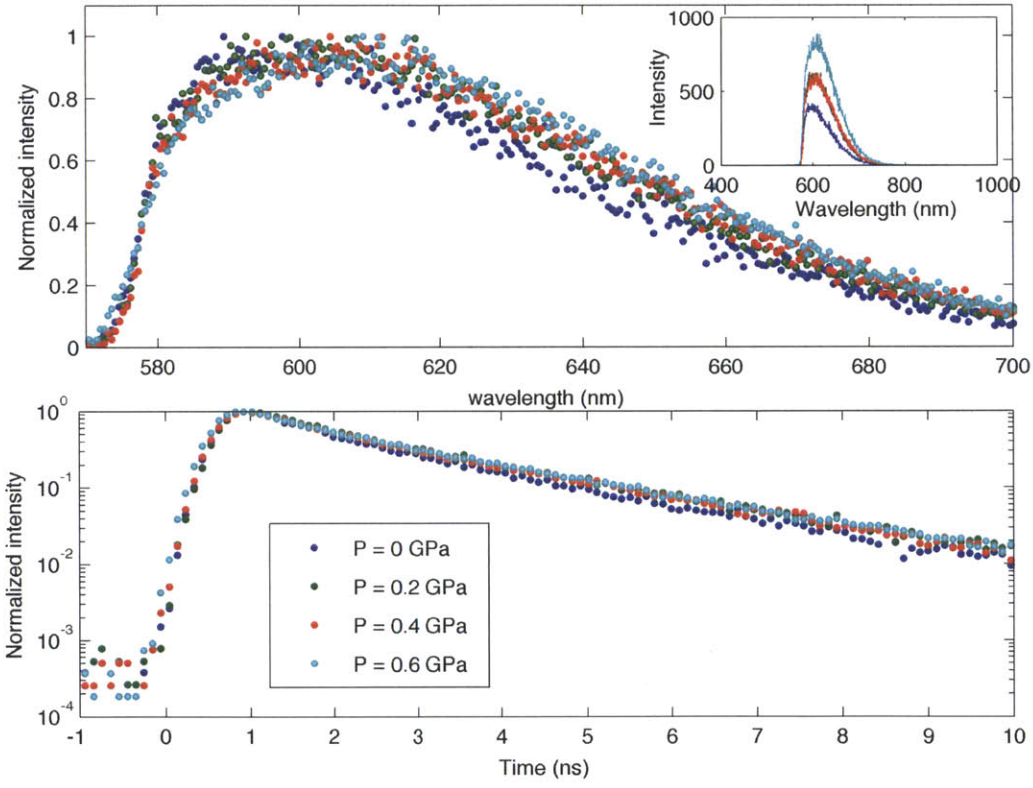

Figure 4-5: Streak camera: time-integrated PL spectra (top) and wavelength-integrated TRPL (bottom) of Alq3:DCM(II) at 1% doping under select pressures. Intensities are normalized for comparison; inset in top figure is the time-integrated PL spectrum with un-normalized intensities.

The integrated data analysis of Alq3:DCM(II) yielded similar results as the PS:DMC(II) films. A similar red shift in spectrum is observed, and lifetime changes were minimal. Because Alq3 is a polar medium, the following analysis of spectral diffusion focused mainly on PS samples.

4.3 Spectral Diffusion

The advantage of using a streak camera over a simple photo-detector setup in observing TRPL is the simultaneous time-resolved and spectrally resolved measurement capability. Thus, it was useful in tracking any change in PL spectrum over time, namely spectral diffusion as the exciton relaxed to lower excited energy states during a short time between excitation and emission. The focus of this section is on the spectral diffusion of PS:DCM(II) films and comparison of the effects of pressure verses doping techniques. This information was extracted from the TRPL streak camera data such as those shown in Figure 4-2 by taking each temporal slice and finding the peak of the emission spectrum at each specific time after excitation. This analysis was performed for each set of data, and plotted as peak emission energy as a function of time in Figure 4-6 for select pressures.

The spectral diffusion rate was found for each set of measurements by fitting a line to the peak energy shift during the first nanosecond after excitation and is listed in Table 4.1. To clarify the effect of pressure, the relative increase in diffusion rate was found by normalizing the diffusion rate to that measured under zero pressure. The relative diffusion rate scale factor is also listed.

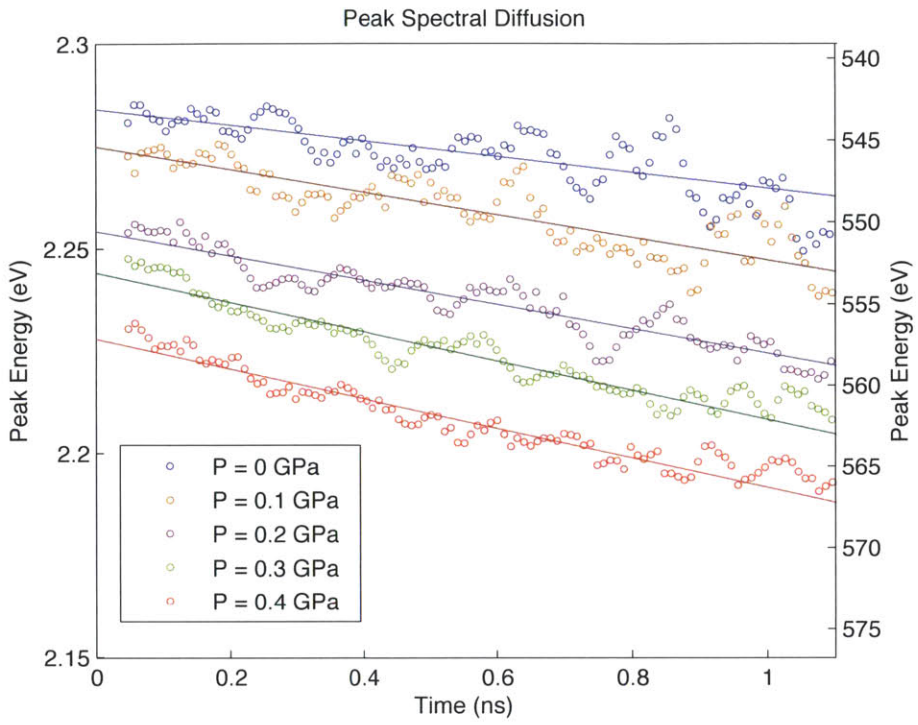

Figure 4-6: Streak camera: spectral diffusion as measured by peak PL emission for PS:DMC(II) wt0.5% under select pressures.

Pressure (GPa)	Lifetime (ns)	Spectral Diffusion Rate (eV/ns)	Relative Rate Factor
0	1.24± 0.04	-0.019± 0.004	1
0.1± 0.1	1.22± 0.02	-0.028± 0.004	1.43
0.2± 0.1	1.28± 0.02	-0.030± 0.003	1.55
0.3± 0.1	1.30± 0.03	-0.035± 0.002	1.84
0.4± 0.1	1.35± 0.03	-0.036± 0.002	1.90

Table 4.1: Fitted lifetime, spectral diffusion rate, and rate factor for select pressures. The relative rate factors are found by normalizing each fitted spectral diffusion rate to the no pressure.

Since the Frenkel exciton energy transfer in these organic thin films occur through Forster radiative energy transfer (FRET) [34, 35], the change in spectral diffusion rate is expected. The change in spectral diffusion rate under compression is due to two major processes. First, under pressure, the intermolecular spacing between the solvent and the solute dye decreases, thus the spacing between the sparsely doped DCM(II) dye molecules, r, also decreases proportionally. Since FRET transfer rate scales as $k_{FRET} \propto \frac{1}{r^6}$, we expect a increase in transfer rate. Second, assuming a constant FRET radius r_{FRET}, as more molecules are packed closer, the number of available transfer sites also increases. Both factors contribute to an overall increase in the magnitude of spectral diffusion rate.

Consider only the effect of change in molecular density on FRET rate, which is estimated from pressure and the fitted elastic modulus of 1.2 GPa for PS. Similar theoretical relative scale factors on the FRET rate were computed and compared with the corresponding scale factor on spectral diffusion rate in Figure 4-7.

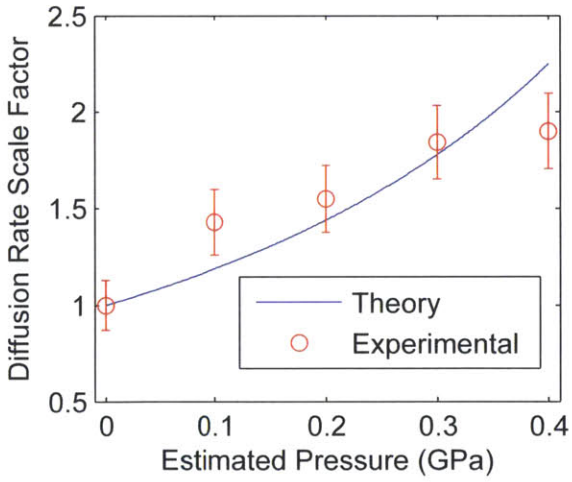

Figure 4-7: Relative Spectral diffusion rate (dot) compare to FRET rate $\frac{1}{r^6}$ factor (solid line) due to change in dye density.

To compare these pressure result, the same spectral TRPL measurements and analysis were performed on films of PS:DCM(II) at varying doping concentration by weight. The measured spectral diffusion is plotted in Figure 4-8.

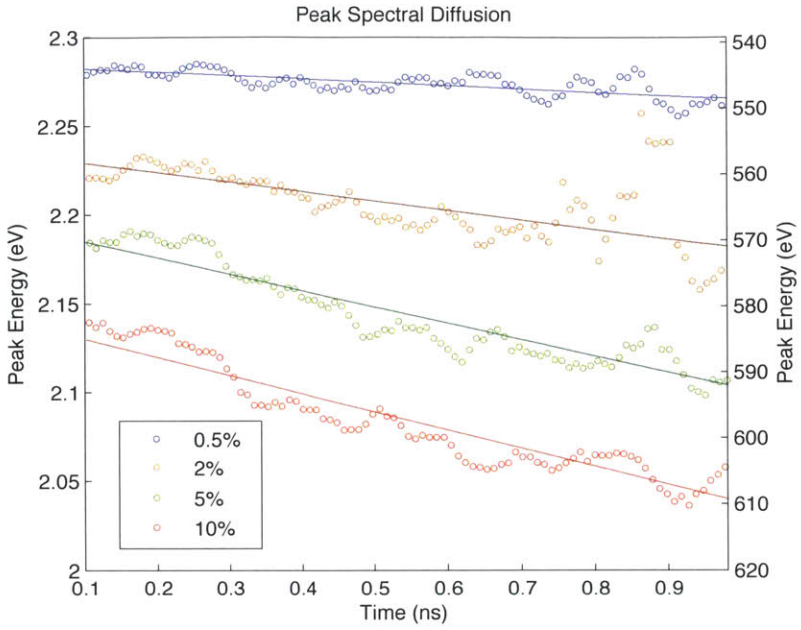

Figure 4-8: Streak camera: spectral diffusion as measured by peak PL emission for PS:DMC(II) with a range of doping concentration by percent weight.

The fitted diffusion rates and relative rate scale factors are listed in Table 4.2.

Doping (wt%)	Spectral Diffusion Rate (eV/ns)	Relative Rate Factor
0.5	-0.019± 0.004	1
2	-0.048± 0.011	2.5
5	-0.096± 0.006	5.0
10	-0.103± 0.007	5.4

Table 4.2: Spectral diffusion rate and rate factor for select doping concentrations.

Although a larger change in the spectral diffusion rate is observed for the doping method than for sample under pressure, the doping analysis is not as simple. The same simple comparison to the FRET rate is no longer valid since a 10% doped film by dye molecule density consideration should have 400 times the rate of of 0.5% doped film, which is significantly different from the observed factor of 5.4.

Chapter 5

Application to Exciplex System

Any technique that reveals some property of the physical world is important. However, the importance stems from an application of that understanding or technique that could advance current technology. One relevant application of organic films studied this thesis is in the form of OLEDs. OLEDs have been commercially successful partly due to ease of fabrication, device flexibility, and range of color availability. In this section, we discuss preliminary work on organic material systems for more efficient OLEDs. The system under consideration is a blend bulk heterojunction of 4,4',4"-Tris(N-3-methylphenyl-N-phenylamino)triphenylamine (m-MTDATA) and Tris(2,4,6-trimethyl-3-(pyridin-3-yl)phenyl)borane (3TPYMB).

5.1 Background

The interfaces formed by m-MTDATA (hole-injection layer) and 3TPYMB (electron-injection layer) create exciplex states, which are a form of charge-transfer (CT) states. A CT state involves an exciton delocalized across 2 different molecules; in this case, the bound electron is localized on the 3TPYBM, while the corresponding hole is on the m-MTDATA. This bound state is an intermediary between free charge states and exciton states. In OLEDs, this exciplex eventually recombines and emits a photon of the energy difference between the lowest unoccupied molecular orbit (LUMO) of the electron-injection layer and the highest occupied molecular orbit (HOMO) of the

hole-injection layer (Figure 5-1). Most OLEDs suffer from the unfortunate property that 75% of created excitons exist in the non-radiative triplet state. Since only the singlet state is quantum mechanically allowed to transition to ground state, emission is somewhat limited to the 25% singlet excitons. Previous work on phosphorescent OLEDs used doped films to assist spin-orbit coupling in order for the triplet exciton to transfer into singlet before emitting in delayed fluorescence. [36, 37].

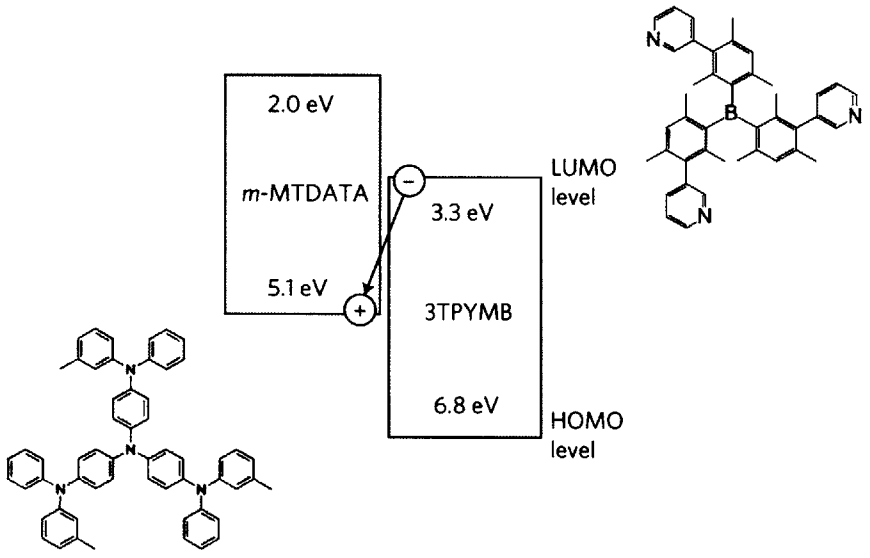

Figure 5-1: Illustration of CT state recombination in energy diagram of m-MTDATA and 3TPYMB and respective chemical structures [2].

However, there is a lack of a clear understanding of the mechanism and rates of intersystem crossing (ISC) from singlet to triplet and reverse intersystem crossing (RISC) from triplet to singlet. We propose the SSSE via pressure method of tuning exciton energies, both singlet and triplet, which may change the energy splitting between the two states. Due to the nature of the exciples state, tuning the distance between the two different molecules will change the spatial overlap and alter the delocalization of the exciton across the molecules, which should also change the energy splitting. Note that transition between ground state and triplet state is quantum mechanically forbidden. Thus, all emission and absorption transition occurs between the ground state and the singlet state.

This material system has the characteristics of a clear prompt PL fluorescence (emission directly from singlet state) and a significant delayed fluorescence (emission from the singlet state after ISC and RISC). Due to the time necessary for the exciton to transfer from the initially excited singlet to triplet, then back to singlet before emission, the lifetime of the delayed fluorescence is orders of magnitude longer than that of the prompt. Recent work on m-MTDATA:3TPYMB and similar OLED systems demonstrated the importance of temperature on thermally assisted delay fluorescence (TADF) on OLED emission [2]. Since the RISC pathway is a thermally-assisted process, the change in temperature determined the thermal energy available to help the triplet exciton to overcome the energetic barrier of the splitting. This was observed in an increase in RISC rate as measured by delayed PL fluorescent lifetimes for increasing sample temperature. However, similar measurements could be performed under pressure, and may yield interesting results and a better physical understanding of the system.

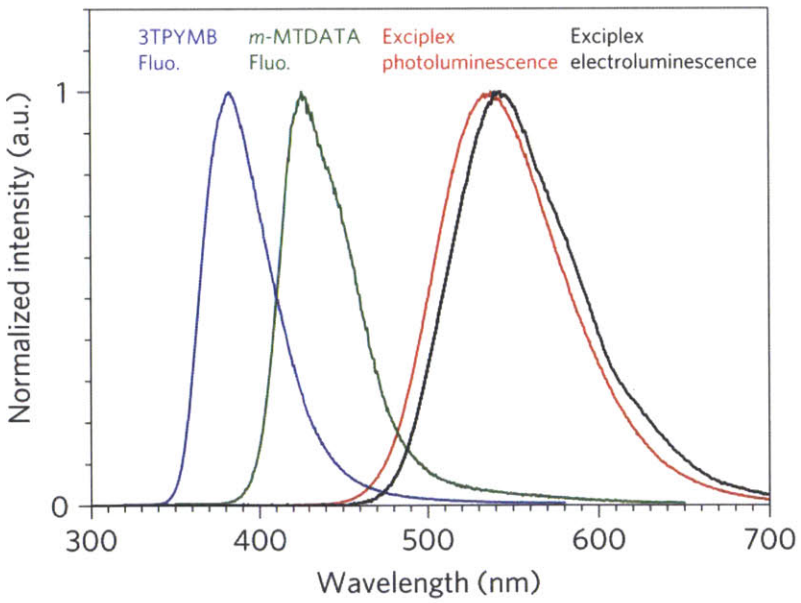

Figure 5-2: PL emission spectra of 3TPYMB, m-MTDATA, and exciplex emission, both PL and EL [2].

5.2 Exciplex Samples

Samples were prepared in a similar manner as the PS:DCM(II) films. The bulk heterojunction film is formed by dissolving the organics at 1:1 ratio in chloroform and spin-coating from solution onto glass. To reflect excitation light and increase signal to noise ratio, a 100 nm layer of Ag is evaporated on top of organic film before packaging with a thin glass cover using epoxy to prevent photo-oxidation. Figure 5-2, from literature [2], shows the PL of each constituent material and the exciplex emission. As expected the exciplex emission energy is much lower than the energy band gap of each material. As consistent with other OLEDs, the electroluminescence (EL) is slightly red shifted from PL due the Stark effect of the external electric field applied to operate the OLED.

5.3 Steady-State PL

Using 200 ps laser excitation of 400 nm to create excitons in m-MTDATA, the excited singlet excitons have to diffuse to an interface in order to emit as an exciplex. At the interface, it may directly emit, ISC and RISC to triplet, or relax in non-radiative pathways from either the singlet or triplet state. We measured the exciplex PL emission in both sample and pressure scans. Similar to the previous thin film work, the results showed a clear red shift in peak wavelength of the emission. Figure 5-3 shows a typical sample scan across the point of compression with computed peak and centroid.

It is interesting to note the change in intensity of the emission under pressure as well as the spectral shift. To fully consider all the parameters in measuring small changes in intensity, factors such as light coupling into the detection fiber and laser fluctuations needed to be considered. Thus, a small amount of pick off laser light was coupled into the same fiber. Since the laser was spectrally separated from the signal, each spectral intensity was normalized to corresponding laser excitation intensity. Figure 5-4 shows a typical raw data pressure scan with laser residue.

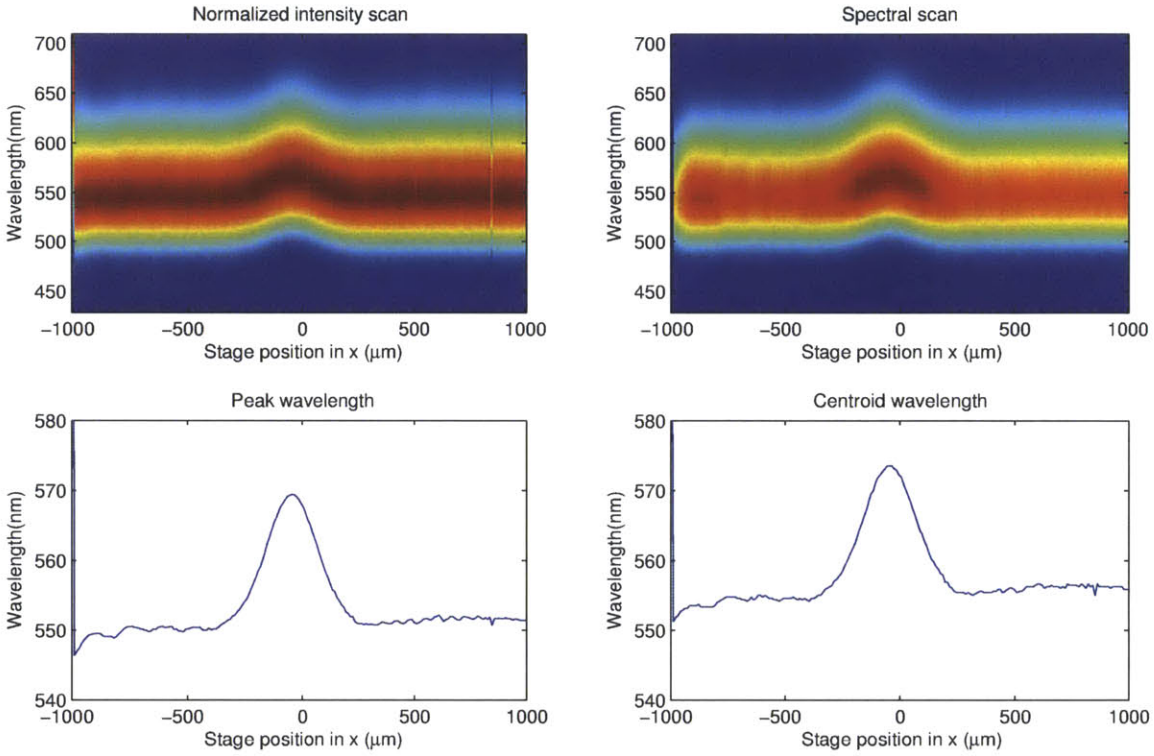

Figure 5-3: Exciplex PL sample scan: (top-left) with color scaled intensity normalized to the peak of each spectrum, (top-right) un-normalized intensity to show a slight change in emission intensity under pressure, (bottom-left) computed peak wavelength of each spectrum, (bottom-right) computed centroid wavelength of each spectrum.

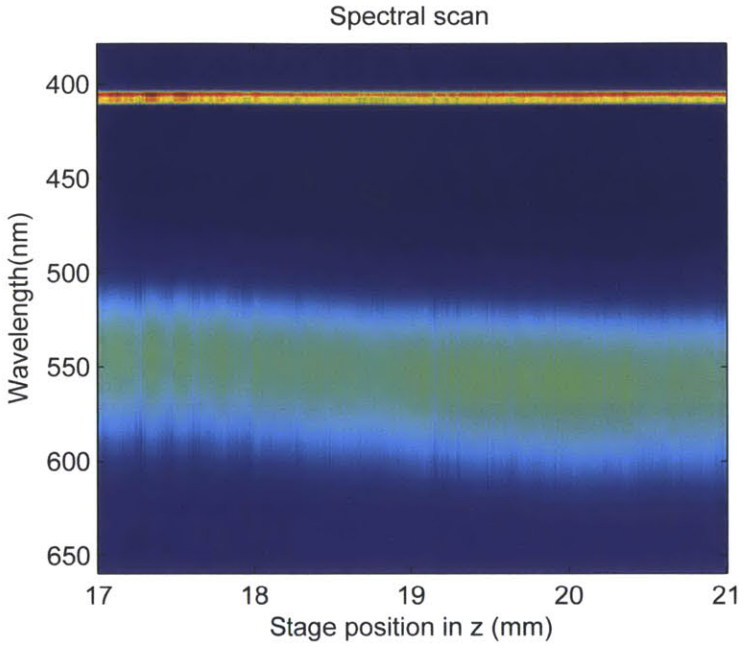

Figure 5-4: Exciplex PL pressure scan. Emission spectral (around 550 nm) intensity as indicated by color-scale is plotted verses wavelength for each micrometer position in z. The residue laser (around 410 nm) shows slight fluctuations during the measurement.

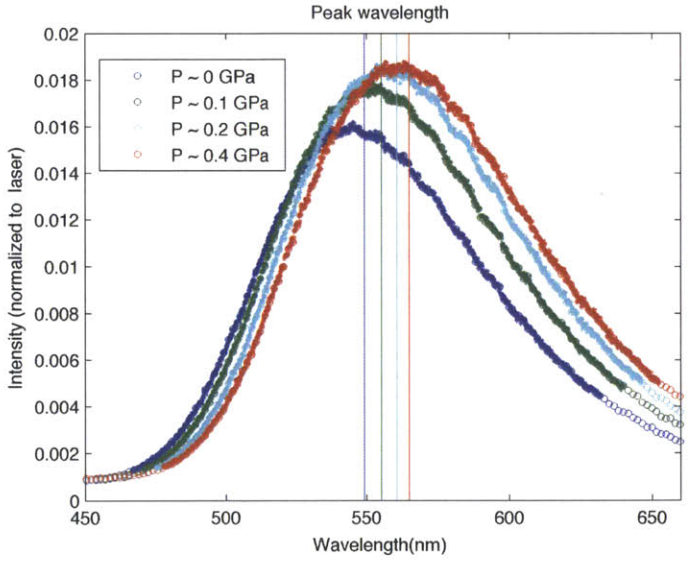

Figure 5-5: Exciplex PL emission spectrum under select pressure. Each set of data is normalized to the corresponding excitation laser intensity.

To compare the emission spectrum under pressure, a plot of the laser-normalized spectral emission for a range of pressures is shown in Figure 5-5.

This shows an increase in the exciplex PL emission peak intensity as well as the characteristic SSSE red shift for increasing pressure. Taking the integral of the laser-normalized spectrum gives the integrated PL intensity for each pressure. We can normalize the PL intensity to that measured under zero pressure to clearly see any intensity increase due to pressure. Figure 5-6 shows this integrated PL intensity factor for several scans. Both compression and release of compression scans shows a clear change in the emission intensity as a function of applied pressure.

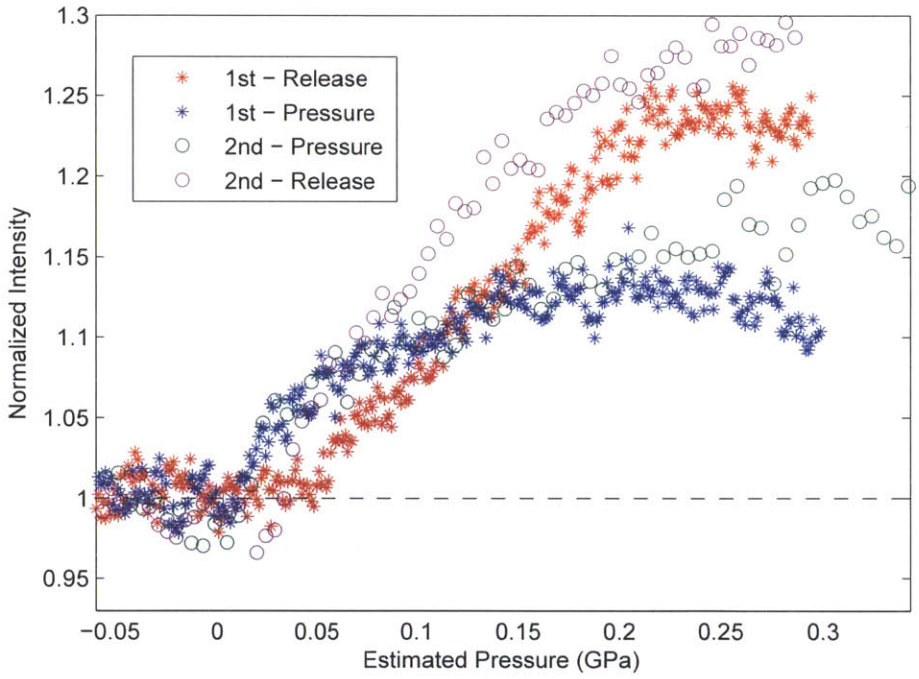

Figure 5-6: PL integrated intensity as a function of pressure for two independent scans. "Pressure" indicates measurements taken during compression from zero pressure. "Release" indicates measurements taken from high pressure to zero pressure.

The data suggest some type of hysteresis in either or both the mechanical setup and film packing density. Since the films were spin coated, the film may be more densely packed after initial compression. This slight difference between compression and the release of pressure may be an interesting point of further investigation. Nev-

ertheless, the increase in emission intensity is consistent between measurements. This increase in intensity can be understood as a change in the ISC or RISC rates due to pressure, which creates a larger singlet emission population.

5.4 TRPL

Since the delayed fluorescence of the exciplex is a significant portion of the total emission, TRPL is a essential measurement for understanding the changes in the exciplex system. The streak camera was employed to measure the exciplex emission and the laser pick-off or residue intensity simultaneously. Measurements were taken mainly using two time ranges: 5 ns and 10 us, to measure the lifetime of the prompt and delayed fluorescence, respectively.

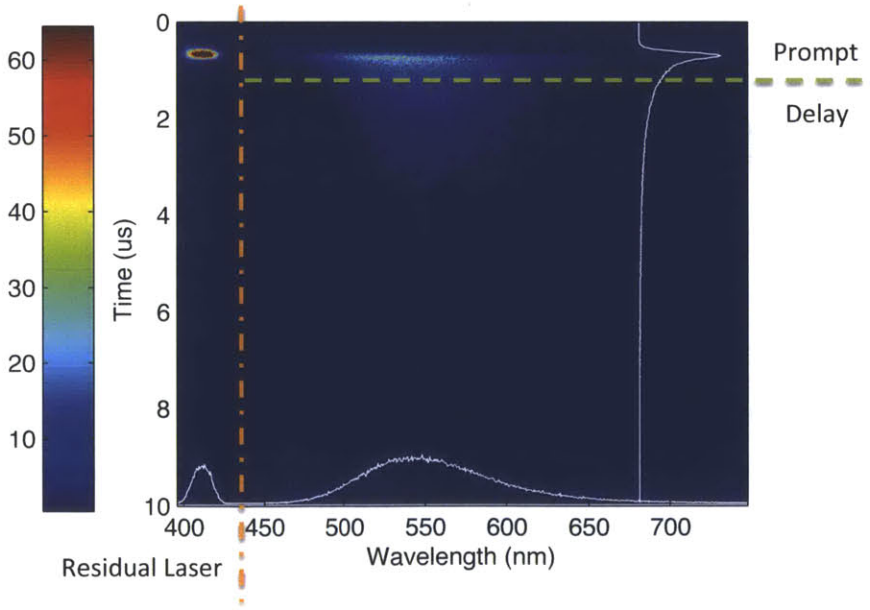

Figure 5-7: Typical exciplex PL emission measured by the streak camera: laser residue (around 400nm), prompt fluorescence on the scale of nanoseconds, and long delay fluorescence on microsecond scale.

5.4.1 Lifetime

The wavelength integrated TRPL from the streak camera data for m-MTDATA:3TPYMB under pressure showed interesting results in changes of both prompt and delay exponential lifetime. A simplified model would involve a bi-exponential function fit for both the prompt and delay fluorenscent. However, since the data was taken with specific time ranges, a single exponential fit to the relevant time range suffices. As shown in Figure 5-8, the prompt fluorescence lifetime was found by fitting to the range of 1.5 ns to 4.5 ns after excitation. The integrated TRPL is plotted as dots and the dotted lines indicate the fitted lifetime for the corresponding colors.

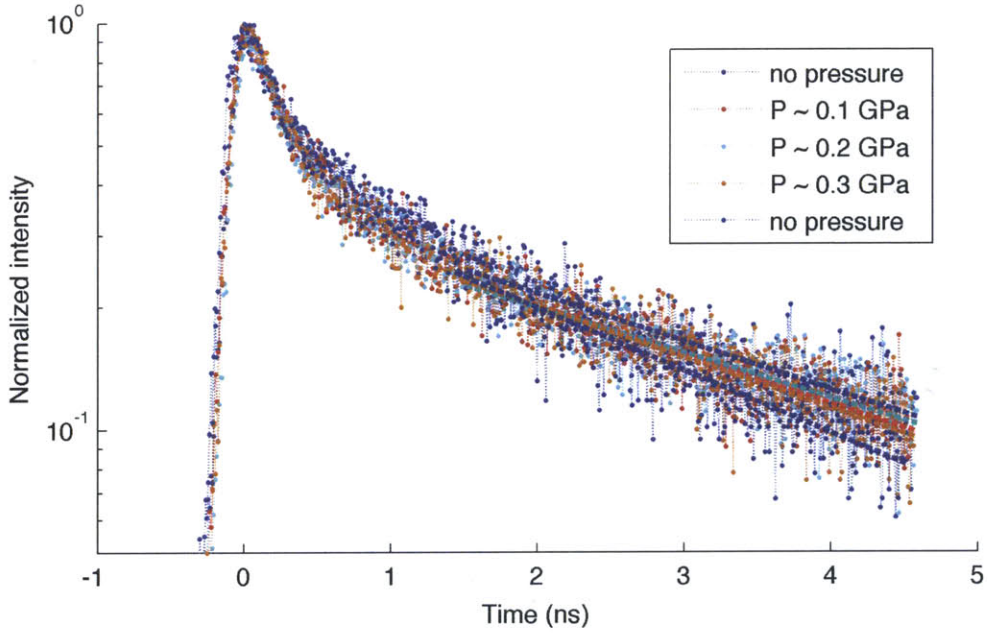

Figure 5-8: Log scale plot of TRPL of the prompt fluorescence of m-MTDATA:3TPYMB sample under pressure. The dotted line fits the relevant time range for the correspondingly colored data.

Shown in Figure 5-9, the delayed fluorescence lifetime was found by fitting to the range of 5us to 9us after excitation. Similarly, the dotted line fitted the correspondingly colored TRPL.

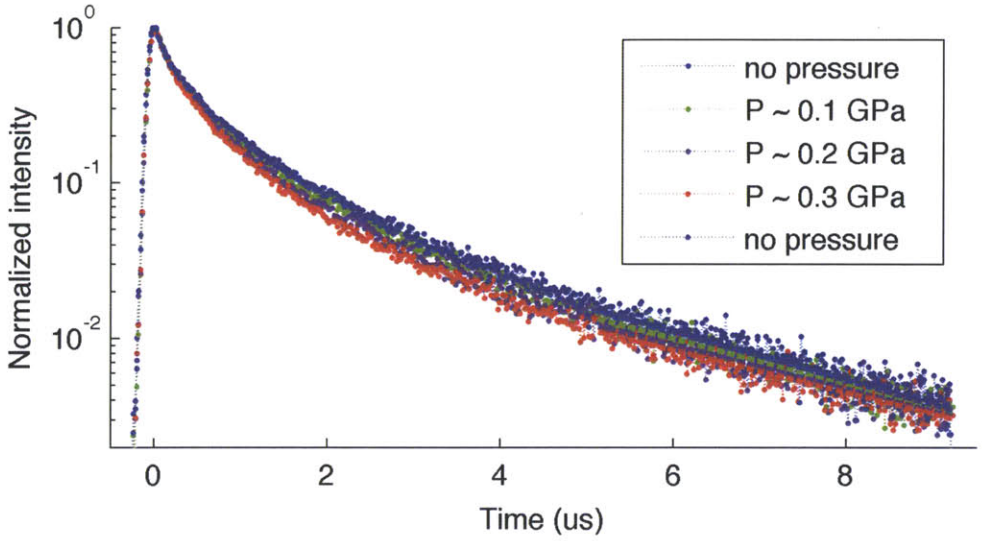

Figure 5-9: Log scale plot of TRPL of the delayed fluorescence of m-MTDATA:3TPYMB sample under pressure, with dotted line fitting the relevant time range for the correspondingly colored data.

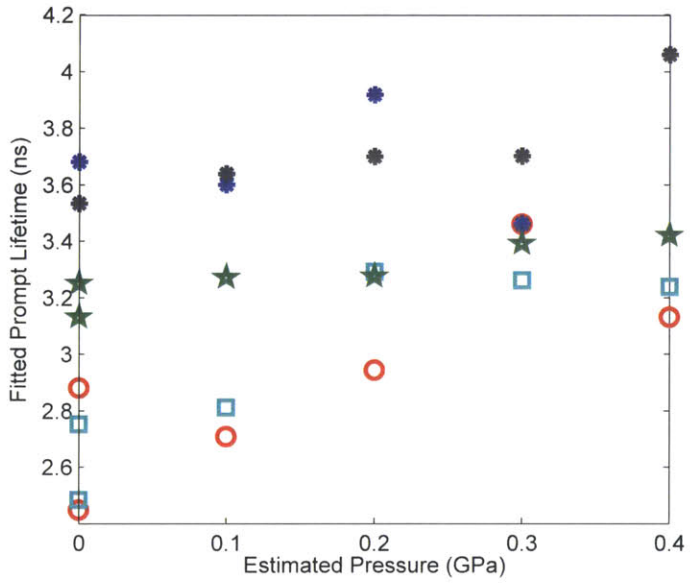

Figure 5-10: Fitted prompt lifetime from TRPL data as a function of estimated pressure for several independent scans as indicated by different symbols and colors. A slight increasing trend in lifetime as a function of pressure is observed.

Notice that the prompt fluorescence is also recorded in the longer time window

(10 μs), but due to instrument response, the time resolution for longer time windows does not allow precise measurement of the prompt TRPL. Figure 5-10 and Figure 5-11 display the fitted prompt and delay lifetimes, respectively, as a function of estimated pressure for several independent measurements.

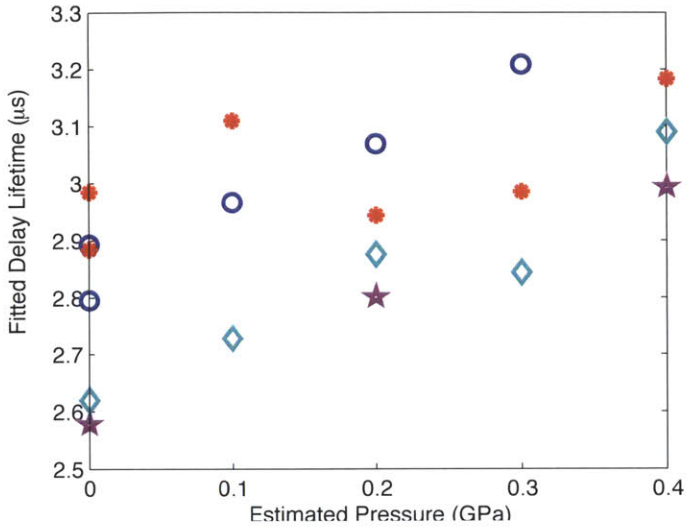

Figure 5-11: Fitted delay lifetime as a function of estimated pressure for several independent scans as indicated by different symbols and colors.

The increase in the delay lifetime suggests a change in ISC or RISC rate between the singlet-triplet coupling under pressure, indicative of a change in the excitonic overlap between the two states. The slight increase in the prompt fluorescent lifetime suggests a change in the singlet radiative process, or a change in the ISC and RISC rates, or both.

These changes in the rate factor due to compression prompt further investigation into the change in relative intensity of emission. The experiments necessitate a theoretical model of exciplex energetics under compression and a full understanding of the rate model involved. Further investigation in the time-resolved exciplex emission under pressure, both PL and EL, could provide useful insight for device physics and optimization methods.

Chapter 6

Conclusion

This thesis presented and demonstrated a viable method of probing local dielectric field effects in organic thin films using a pressure method. We considered the theoretical implications on PL emission of organic films under compression. A simplified solvation effect expression was derived based on liquid state modeling to fit experimental data of change peak emission energy as a function of pressure.

Films of low doping concentration of DCM(II) dye in both polar (Alq_3) and non-polar (PS) media were experimentally tested for SSSE under pressure. Over 20 nm red shift in peak and centroid PL emission was observed for Alq_3:DCM(II) films under $\sim$0.4 GPa, and a similar 10 nm shift was observed for PS:DCM(II) films. The observed bathochromic shift in peak PL emission is consistent with the simplified OLM theory, and an approximate elastic modulus for each medium was obtained as a fitting parameter.

To further quantify the effects of compression, spectral TRPL measurements were taken with a streak setup. The fitted exponential lifetimes of excitons in organic films under pressure did not change appreciably as compared to similar measurement take for films with variable doping. This indicates no aggregation effects of compression, unlike tuning exciton energy by increasing solute doping, which results in a change in lifetime due to exciton trapping and quenching at aggregation sites.

The spectral diffusion measurements for PS:DCM(II) films for both pressure and doping methods were performed and quantified. The fitted spectral diffusion rate of

the sample under compression was found to be reasonable with the SSSE predicted molecular density. Although large diffusion rate variability was observed through increasing dye doping, the change in diffusion rate was no longer comparable to the corresponding dye density.

In conclusion, the pressure method is arguably a simpler method of understanding SSSE than the accepted doping methods. It eliminated composition effects and sample to-sample variability. The propose compression method provides an external parameter to fine tune exciton energetics and could prove to be a useful tool in future studies such as exciton diffusion and device optimization.

6.1 Future work

Preliminary pressure experiments on exciplex emission from a bulk heterojunction OLED system were performed and indicated changes in prompt and delay lifetimes as well as PL emission intensity. Further work is planned to investigate the change in PL intensity from prompt and delay fluorescence. These experiments could provide insights into device physics and applications if techniques such as pre-stressed deposition could improve efficiencies.

A new pressure system to provide *in situ* measurements of the film thickness under compression would greatly improve the technique, and remove some assumptions made in theoretical work. Further applications on device measurements could give better physical understanding for optimization. The addition of electrical contacts to devices under pressure and optical excitation could allow further testing of devices such as solar cells and OLEDs under operation. The current setup is electrical probe compatible, but error in applied pressure could be a difficulty. Future improvements on technologies such as diamond anvil cells could allow integration of electrical contacts for the purpose of pressure testing optoelectronic devices.

Bibliography

[1] V. Bulović, R. Deshpande, M. E. Thompson, and S. R. Forrest, "Tuning the color emission of thin film molecular organic light emitting devices by the solid state solvation effect," *Chemical Physics Letters*, vol. 308, pp. 317–322, 1999.

[2] K. Goushi, K. Yoshida, K. Sato, and C. Adachi, "Organic light-emitting diodes employing efficient reverse intersystem crossing for triplet-to-singlet state conversion," *Nature Photonics*, vol. 6, no. April, 2012.

[3] R. Capelli, S. Toffanin, G. Generali, H. Usta, A. Facchetti, and M. Muccini, "Organic light-emitting transistors with an efficiency that outperforms the equivalent light-emitting diodes.," *Nature materials*, vol. 9, pp. 496–503, June 2010.

[4] J. Weidner, *Organic Semiconductor Materials and Devices: ECS Transactions: Volume 11.* The Electrochemical Society, 2008.

[5] A. P. Green, K. T. Butler, and A. R. Buckley, "Tuning of the emission energy of fluorophores using solid state solvation for efficient luminescent solar concentrators," *Applied Physics Letters*, vol. 102, no. 13, p. 133501, 2013.

[6] M. J. Currie, J. K. Mapel, T. D. Heidel, S. Goffri, and M. A. Baldo, "High-efficiency organic solar concentrators for photovoltaics.," *Science (New York, N.Y.)*, vol. 321, pp. 226–8, July 2008.

[7] S. I. Hintschich, H. Gothe, V. G. Lyssenko, H. Fröb, and K. Leo, "The effects of inhomogeneous broadening in an organic microcavity laser," *Optical and Quantum Electronics*, vol. 40, pp. 397–402, July 2008.

[8] M. Koschorreck, R. Gehlhaar, V. G. Lyssenko, M. Swoboda, M. Hoffmann, and K. Leo, "Dynamics of a high-Q vertical-cavity organic laser," *Applied Physics Letters*, vol. 87, no. 18, p. 181108, 2005.

[9] V. Bulović, A. Shoustikov, M. Baldo, E. Bose, V. Kozlov, M. Thompson, and S. Forrest, "Bright , saturated , red-to-yellow organic light-emitting devices based on polarization-induced spectral shifts," *Chemical Physics Letters*, vol. 287, no. May, pp. 455–460, 1998.

[10] Z. Guo, W. Zhu, and H. Tian, "Dicyanomethylene-4H-pyran chromophores for OLED emitters, logic gates and optical chemosensors.," *Chemical communications (Cambridge, England)*, vol. 48, no. 49, pp. 6073–84, 2012.

[11] T. Someya, T. Sekitani, S. Iba, Y. Kato, H. Kawaguchi, and T. Sakurai, "A large-area, flexible pressure sensor matrix with organic field-effect transistors for artificial skin applications.," *Proceedings of the National Academy of Sciences of the United States of America*, vol. 101, pp. 9966–70, July 2004.

[12] M. Sougawa, K. Takarabe, Y. Mori, T. Okada, T. Yagi, H. Kariyazaki, and K. Sueoka, "Bulk modulus and structural changes of carbon nitride C2N2(CH2) under pressure: The strength of CN single bond," *Journal of Applied Physics*, vol. 113, no. 5, p. 053510, 2013.

[13] H. Li and J. J. Vlassak, "Determining the elastic modulus and hardness of an ultra-thin film on a substrate using nanoindentation," *Journal of Materials Research*, vol. 02138, no. November 2008, pp. 1114–1126, 2009.

[14] O. Berg and E. L. Chronister, "Optical dephasing in pentacene-doped PMMA under high pressure Optical dephasing in pentacene-doped PMMA under high pressure," *The Journal of Chemical Physics*, vol. 4401, no. 106, 1997.

[15] M. Chandrasekhar, S. Guha, and W. Graupner, "Squeezing Organic Conjugated Molecules What Does One Learn?," *Advanced Materials*, vol. 13, no. 8, pp. 613–618, 2001.

[16] Z. Rang, M. I. Nathan, P. P. Ruden, R. Chesterfield, and C. D. Frisbie, "Hydrostatic-pressure dependence of organic thin-film transistor current versus voltage characteristics," *Applied Physics Letters*, vol. 85, no. 23, p. 5760, 2004.

[17] J. P. Schmidtke, R. H. Friend, and C. Silva, "Tuning interfacial charge-transfer excitons at polymer-polymer heterojunctions under hydrostatic pressure.," *Phys Rev Lett*, vol. 100, no. 15, p. 157401, 2008.

[18] C. F. Madigan and V. Bulović, "Solid state solvation in amorphous organic thin films.," *Physical Review Letters*, vol. 91, no. 24, p. 247403, 2003.

[19] S. Cha, M. G. Choi, H. R. Jeon, and S.-K. Chang, "Negative solvatochromism of merocyanine dyes: Application as water content probes for organic solvents," *Sensors and Actuators B: Chemical*, vol. 157, pp. 14–18, Sept. 2011.

[20] M. Meyer and J. Mialocq, "Ground State and Singlet Excited State of Laser Dye DCM: Dipole Moments and Solvent Induced Spectral Shifts," *Optics Communicaitons*, vol. 64, no. 3, pp. 264–268, 1987.

[21] L. Onsager, "Electric Moments of Molecules in Liquids," *Journal of the American Chemical Society*, vol. 58, pp. 1486–1493, 1936.

[22] A. Marini, A. Munoz-Losa, A. Biancardi, and B. Mennucci, "What is Solvatochromism?," *The Journal of Physical Chemistry B*, vol. 114, pp. 17128–17135, 2010.

[23] Y. Ooshika *J. Phys. Soc. Jpn.*, no. 9, p. 594602, 1954.

[24] Y. K. M. Mataga and M. Koizumi *Bull. Chem. Soc. Jpn.*, no. 28, p. 690, 1955.

[25] E. Z. Lippert *Naturforsch.*, no. 10A, p. 541, 1955.

[26] J. Lakowicz, *Principles of fluorescence spectroscopy.* Springer London, Limited, 2009.

[27] C. Reichardt, *Solvents and Solvent Effects in Organic Chemistry.* Wiley, 2006.

[28] V. G. Kozlov, G. Parthasarathy, P. E. Burrows, V. B. Khalfin, J. Wang, S. Y. Chou, and S. R. Forrest, "Structures for Organic Diode Lasers and Optical Properties of Organic Semiconductors Under Intense Optical and Electrical Excitations," *IEEE Journal of Quantum Electronics*, vol. 36, no. 1, pp. 18–26, 2000.

[29] K. Miyake, N. Satomi, and S. Sasaki, "Elastic modulus of polystyrene film from near surface to bulk measured by nanoindentation using atomic force microscopy," *Applied Physics Letters*, vol. 89, no. 3, p. 031925, 2006.

[30] J. M. Torres, N. Bakken, C. M. Stafford, J. Li, and B. D. Vogt, "Thickness dependence of the elastic modulus of tris(8-hydroxyquinolinato)aluminium," *Soft Matter*, vol. 6, no. 22, p. 5783, 2010.

[31] N. Bakken, J. M. Torres, J. Li, and B. D. Vogt, "Thickness dependent modulus of vacuum deposited organic molecular glasses for organic electronics applications," *Soft Matter*, vol. 7, no. 16, p. 7269, 2011.

[32] R. Balili, V. Hartwell, D. Snoke, L. Pfeiffer, and K. West, "Bose-Einstein condensation of microcavity polaritons in a trap.," *Science (New York, N.Y.)*, vol. 316, pp. 1007–10, May 2007.

[33] A. Uddin and C. B. Lee, "Exciton behaviours in doped tris (8-hydroxyquinoline) aluminum (Alq3) films," *Physica Status Solidi (C)*, vol. 8, pp. 80 83, Jan. 2011.

[34] T. Förster, *Intermolecular energy transfer and fluorescence.* National Research Council of Canada, 1955.

[35] F. Fennel and S. Lochbrunner, "Förster-mediated spectral diffusion in disordered organic materials," *Physical Review B*, vol. 85, p. 094203, Mar. 2012.

[36] S. Kappaun, C. Slugovc, and E. J. List, "Phosphorescent organic light-emitting devices: working principle and iridium based emitter materials.," *International journal of molecular sciences*, vol. 9, pp. 1527–47, Aug. 2008.

[37] M. A. Baldo, D. F. O. O'Brien, Y. You, A. Shoustikov, S. Sibley, M. E. Thompson, and S. R. Forrest, "Highly efficient phosphorescent emission from organic electroluminescent devices," *Nature*, vol. 395, no. September, pp. 151–154, 1998.